

MECHANOELECTRIC TRANSDUCTION :
A REVIEW AND A METHODOLOGIC APPROACH
TO EXPLAIN THE PHENOMENA

Bogazici University Library



by

Mustafa Karamanoglu

B.S. in M.E., Istanbul Technical University, 1983

Submitted to the Biomedical Engineering
Institute in partial fulfillment of the
requirements for the degree of

Master of Science

in

Biomedical Engineering

Bogazici University

1985

MECHANOELECTRIC TRANSDUCTION :
A REVIEW AND A METHODOLOGIC APPROACH
TO EXPLAIN THE PHENOMENA

APPROVED BY

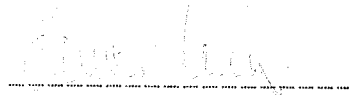
Doc. Dr. Yusuf P. Tan
(Thesis Supervisor)



Prof. Dr. Necmi Tanyolac



Y. Doc. Dr. Omer Cerid



ACKNOWLEDGEMENT

I would like to express my deepest gratitude to Doc. Dr. Yusuf P.Tan my thesis supervisor, for his suggestions during my thesis and for his kind help during the course of my graduate study.

I would further like to express my thanks to Prof. Dr. Necmi Tanyolac for accepting to be on my thesis committee.

I would also like to express my thanks to Y. Doc. Dr. Omer Cerit for his support during all stages of this study.

I need to express my gratitude to the people whom I met by encouraging me to continue on working on this subject.

ABSTRACT

The phenomena of mechanical to electrical transduction is a common response of nervous tissue. In gathering information from environment these tissues are specialized to responde in a fashion like mechanical to electrical transducer. However, it has been demonstrated that this phenomena is related with the intrinsic behaviour of membrane itself and observed in different membrane preparations.

In this thesis a rewiev of the phenomena and models proposed by other investigators is made and a model which seems to explain it is proposed. In order to test the predictions of model, an experimental setup and a methodological approach to conduct the experiment is presented and suggestions are made for future work on this subject.

ÖZETÇE

Mekanik uyarıların elektriksel dönüşümü sinir dokusunun ortak bir özelliğidir. Çevreden bilgi alışverişi sırasında bu dokular bir mekanik-elektrik dönüştürücü gibi davranmaktadırlar. Ancak, bu olayın zarın yapısından doğan bir özelliği olduğu gösterilmiş ve değişik zarlarda gözlemlenmiştir.

Bu tezde olay hakkında var olan bilgiler toplanıp incelenmiş ve olayı açıklayacak bir model ortaya konulmuştur. Modelin ön gördüklerini incelemek için bir deney seti hazırlanıp, deney yöntemleri sunulmuştur.

LIST OF FIGURES

	Page
FIGURE 2.1 Schematic of the experimental arrangement . . .	6
FIGURE 2.2 Peak change in current for mechanical stimulus .	8
FIGURE 2.3 Schematic diagram of the experimental setup. . .	10
FIGURE 2.4.1 Schematic of the experimental setup using patch-clamp technique	12
FIGURE 2.4.2 Schematic representation of the channel embedded in a lipid bilayer layer	14
FIGURE 3.1.1 An idealized view of the red blood cell membrane composite	17
FIGURE 3.1.2 Initiation of excitation	18
FIGURE 3.1.3 Conduction of excitation	19
FIGURE 3.1.4 The formation of the cylinders	19
FIGURE 3.2.1 A membrane model (Na channels)	21
FIGURE 3.2.2 A membrane model (Na currents)	22
FIGURE 3.3.1 The effect of axon stretch	23
FIGURE 3.3.2 Membrane depolarization vs axon stretch.	24
FIGURE 4.1.1 The directional sensivity of the hair cell . . .	26
FIGURE 4.1.2 Copy of an electron-photomicrograph	27
FIGURE 4.1.3 Plunging action of a hair cell	28
FIGURE 4.3.4 Nonuniform extension produced by micropipette aspiration	33
FIGURE 5.2 Experimental arrangement	43
FIGURE 5.2.1.1 Extrusion of axoplasm	45
FIGURE 5.2.1.2 Re-inflation of axon	45
FIGURE 5.2.7 Algorithm for the master program	48

TABLE OF CONTENTS

	Page
ACKNOWLEDGEMENTS	iii
ABSTRACT	iv
OZET	v
LIST OF FIGURES	vi
I. INTRODUCTION	1
II. EXPERIMENTAL SETUPS USED AND FINDINGS	
OBTAINED IN THE PAST	5
2.1 Mechanical Stimulation of Axons	5
2.2 Reversal Potentials Due to Mechanical Stimulation	7
2.3 The Effect of Temporary Increase in Axonal Volume	9
2.4 Mechanosensitive Ion Channel	12
III. THE MODELS PROPOSED TO EXPLAIN THE	
PHENOMENA BY THE FORMER WORKERS	16
3.1 The Transmembrane Macromolecule Rotation Model	17
3.2 The Model of Undercoat and Cytoskeletal Structures Which Supports Na Channels.	18
3.3 The Model of Surface Charge Density Changes	22
3.4 The Model of Piezoelectric Effect Resulting from Mechanical Deformation.	24

IV.	THE PROPOSED MODEL WHICH SEEMS	
	TO EXPLAIN THE PHENOMENA	16
4.1	Morphological Evidences	26
4.2	The Properties of the Receptors	30
4.3	The Possible Models	30
4.3.1	Piezoelectric Effect	30
4.3.2	The Effect of Streaming Potentials	31
4.3.3	The Changes in Surface Charge Density	31
4.3.4	Specific Mechanoelectric Transduction Channel	32
4.3.5	Transmambrane Macromolecule Rotation Model	33
4.4	The Proposed Model of Lipid Rupture	34
4.4.1	Basis of the Model	34
4.4.2	The Model	35
4.4.3	Discussion of the Model	36
4.4.4	Predictions of the Model	39
V.	THE EXPERIMENTAL SETUP TO TEST THE MODEL	41
5.1	Selection of the Experimental Protocol	41
5.1.1	Selection of the Material	41
5.1.2	Selection of the Method to Deliver the Mechanical Stimulus	42
5.1.3	Selection of the Recording System	42
5.1.4	Selection of the Perfusion Solutions	43
5.2	The Experimental Methods	43
5.2.1	Preparation of the Membrane	44
5.2.2	Membrane Fixation Techniques	44
5.2.3	Composition of the Solutions	46

5.2.4	Preparation of Pipettes	46
5.2.5	Data Acquisition	47
5.2.6	Control of Mechanical Pulse Sequence and Data Acquisition	47
VI.	CRITIQUE OF THE METHOD	49
APPENDIX A	51
APPENDIX B	54
APPENDIX C	55
APPENDIX D	57
APPENDIX E	63
APPENDIX F	69
BIBLIOGRAPHY	72

I. INTRODUCTION

Any kind of external stimulus which may be in the form of chemical, mechanical, or electromagnetic energy is transformed into electrical energy by exciting certain cells. The form of energy which will be transformed determines the naming of these cells. In general, a group of cells that are excitable by this way are called nerves in higher organisms. In fact nervous tissue can be considered as a transducer and a processor element of a certain kind of excitation. According to the stimuli that one nerve may be excited with, these tissues are named.

Depending on these considerations, one can assume that mechanical to electrical transduction occurs in the mechano-electrical transducer nerve and carried through the nerves to higher centers to be processed.

It has been shown that the transducer and impulse generating processes, in crayfish slowly adapting receptor and in mammalian pacinian corpuscle are separated (Loewenstein W.R., et al 1963). Therefore it is likely to say that in mechanosensitive organs, the mechanical pulses create a generator potential which in turn cause generation of spike activity. Certain evidences also showed that the electrical response to mechanical stimuli may be

a depolarizing or a hyperpolarizing one depending on the site and the way of excitation of a membrane. A study on non-myelinated nerve terminal in Pacinian corpuscle revealed that hyperpolarizing response is produced on compression of the site, while removal of the compression causes the opposite effect, namely depolarization (Nishi K. et al,1968). Another study showed that the mechanical stimulation of the posterior surface of Paramecium evokes a transient hyperpolarization while the anterior surface evokes depolarization for a similar stimulus (Naitoh Y. et al,1972). In baroreceptor nerve of anaesthetized dog, it was shown that the activity of the nerve can be modulated by changing the carotid sinus dimensions (Bergel D.H. et al,1975) while another study demonstrated that the modulation is sensitive to mechanical stimulus near threshold operation (Arndt J.O. et al,1975). In contrast a study on isolated cat muscle spindles in response to sinusoidal stretch revealed that generator potential per unit length change in both primary and secondary endings is a decreasing power function of displacement (Hunt C.C. et al,1980). On the other hand it has been shown that a mechano-electrical transduction occurs in a step-like fashion in vestibular hair cells of the chick which has a conductance of 50 pS (Ohmori H. et al,1985). Taking into consideration ionic events regulating the generator potential in a vertebrate hair cell, it was shown that the generator currents are carried in vivo by K^+ while the channel is in fact nonspecific (Corey D.P. et al,1979).

The above history shows that in different mechanotransducers the generator potential is dependent on stimulus amplitude and site of stimulus where it is introduced. The channel which is

responsible for transduction is non specific for most of the monovalent ions.

Other than these findings, certain experiments showed that the mechano-electrical transduction occurs not only in mechano-electrical transducers (receptors) but also in every kind of nervous tissue. For example rapid, short duration mechanical compression of Lobster giant axons produces a depolarization and an increase in membrane conductance (Julian F.J. et al,1962) while in Myxicola giant axons an all-or-none action potential is generated when the stimulus strength is sufficient (Ganot G. et al,1981). It was reported that stretch causes depolarizing responses in the node of Ranvier of frog myelinated nerve (Gray J.A.B. et al,1954). But in a different preparation it was shown that an increase in intraaxonal pressure causes squid giant axon to respond in a hyperpolarizing way (Terakawa S. et al,1982). On the other hand it is well known that when a pressure is introduced through mammalian dentine layer the dental nerve produces action potential which is processed as pain (Gurkan S.I. et al,1972). Besides these, it has recently been reported that in tissue cultured embryonic chick skeletal muscle there is a stretch-activated ion channel (Guharay F. et al,1984). Different reports also revealed that stretch-induced ion channels were found in different membranes eg. in Xenopus muscle cells (Brehm P. et al,1984) and in frog red blood cells (Hamill D.P. et al,1983).

All these findings indicate that myelinated or unmyelinated peripheral nerve fibres and some skeletal muscles cited, or

briefly, most of the biological membranes of different species respond to mechanical stimulation either by depolarization or hyperpolarization of the membrane potential. Thus it appears that the mechano-electrical transduction process is not specific for specialized nerve structures but is in fact a general property of excitable membranes.

Throughout this thesis, the experimental methods used and the results of the experiments of former workers will be discussed while the theoretical considerations about this phenomena which were discussed elsewhere will be revised. Depending on the results of revision, a theoretical model which seems to explain the phenomena more suitably will be proposed. After this, in order to test the reliability of the model proposed, an experimental setup will be presented.

II. EXPERIMENTAL SETUPS USED AND FINDINGS OBTAINED IN THE PAST

Current records indicate that the past of research on nerve excitability by mechanical stimuli begins with Tigerstedt (Tigerstedt R., 1880).

2.1 Mechanical Stimulation of Axons

It is assumed that the first methodological approach to this phenomena was carried out in 1962 by Julian F.J. et al (Julian & Goldman, 1962). In this approach the authors used lobster giant axon which had approximate diameters of 100 μm for being geometrically simple and relatively free from structures and frog sciatic nerve which was composed of 5 or 6 individual fibres resulting in a final diameter of about 10 μm . They excited the nerve with applying rectangular pulses to a suitably damped Rochelle salt bimorph on which a glass stylus of 1 mm in diameter was mounted. The experimental arrangement used by the authors in this research is given in fig.2.1.

The results of this experiment can be summarized as follows: When the magnitude of stylus displacement was 10 to 15 μm at a velocity of 5 cm/sec an action potential was initiated but if the stimulus was applied in a slower way no depolarization was seen. It has also been observed that a long period of several seconds is needed for full recovery. The difference between the short and long durational mechanical impulses in response nature is that;

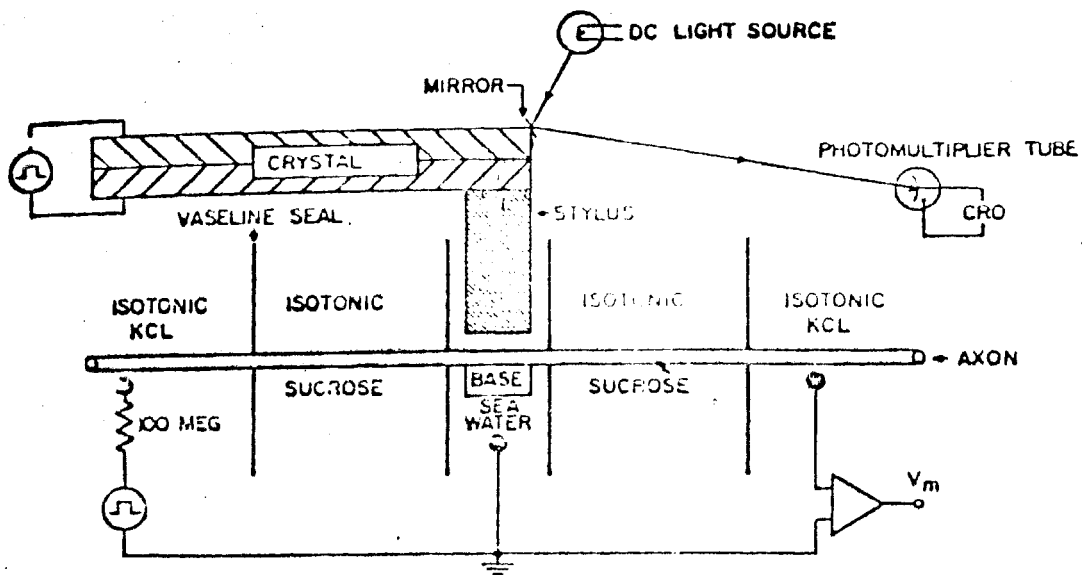


Fig.2.1 Schematic of experimental arrangement. Width of central gap, diameter of glass stylus, and width of base all about $1 \mu\text{m}$. Width of isotonic sucrose pools 2 to $3 \mu\text{m}$. Black, solid circles represent reversible silver-silver chloride electrodes, (from Julian et al, 1962).

during short pulses the recovery was fast whereas in longer durational pulses the recovery was slow. If the extracellular fluid was changed with choline or procaine to replace Na^+ , the response was abolished. With the removal of these chemicals from the medium by washing with artificial sea water, a full recovery was maintained.

In this paper the authors discussed the possible mechanisms by which these findings can be explained and resulted with the following:

- a. The bending of the membrane was unlikely because of the large diameter of the stylus.
- b. Streaming potentials could be disregarded because these would contribute a reversal in sign of the potential change during recovery but such an evidence was not observed.
- c. On the other hand if a compression is introduced to the axon the contents of the region under stylus are distorted and also the resulting stretch causes an increase in membrane area which would cause molecular elements to be separated either uniformly or at certain preferred regions.
- d. The major differences between frog fiber bundle and lobster giant axon are the rapid recovery and occasional off response of the former.

2.2 Reversal Potentials Due to Mechanical Stimulation

Approximately two decades after this experiment, another attempt was made in order to resolve the reversal potentials corresponding to the mechanically-induced conductance increase (Ganot G. et al ,1981).

The obtained reversal potential would show the ionic pathways responsible for this phenomena. In this set of experiments the authors used Myxicola axonal preparation which had an axonal

diameter of 500 μm in conventional voltage clamp conditions. The mechanical pulses were delivered by a loudspeaker which was driven by a power amplifier controlled by a pulse generator. The stylus connected to the loudspeaker had a diameter of 2 mm where the rise time of its movement was 1 msec.

The responses observed with this preparation were summarized as follows : The change in membrane potential induced by a mechanical stimulus depends both on magnitude and the rate of change of the stimulus. The addition of TTX eliminates action potential but does not affect the mechanically induced depolarization. When the axon was clamped to its resting potential, the current response to a mechanical stimulus was an inward current of long duration with an exponential decay time constant of 10 sec. The stimulus magnitude and current-voltage relation curves are given in fig.2.2.

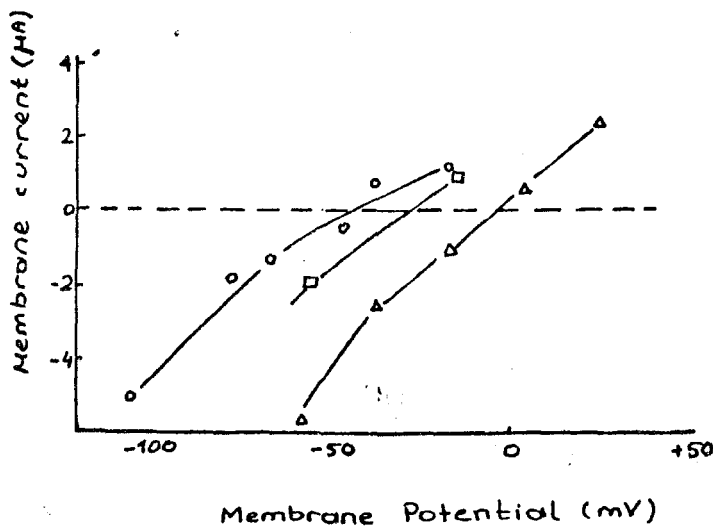


Fig. 2.2 Peak change in current as a function of membrane potential for three different mechanical stimulus amplitudes: 29 μm (circles), 53 μm (triangles), and 60 μm (squares). Stimulus duration 5 ms, (from Ganot et al, 1981).

When TTX and TEA were added the reversal potential for leakage current could be obtained which denoted a reversal potential of -43 mV while a mechanically induced reversal potential gave a value of -46 mV. The close reversal potential values obtained this way were interpreted as the same leakage channels being involved on the both processes.

The discussion made by the authors on these experimental findings concentrated on the hypothesis that the mechanical stimulus dependent excitation does not involve specific channels because if it were so; a predetermined reversal potential would be seen, but instead, it involves leakage channels which are gradually increased with the stimulus strength. For this reason the authors suggested that if the membrane proteins reoriented, some of the lipids form intermittent or stable polar pathways for ionic transport, the mechanically induced conductance would arise from an increase in the average number of such nonspecific pathways, and the change in reversal potential could arise from the increase in their average size.

2.3 The Effect of Temporary Increase in Axonal Volume

One year later in order to understand the mechanism behind this phenomena another study was made (Terakawa S. & Watanabe A., 1982) where the authors used squid (*Doryteuthis Bleekeri*) giant axon.

The method was highly different in mechanical and procedural aspects from the former experiments. They injected a volume of perfusion fluid intracellularly when the axon was in voltage clamp conditions. The original experimental setup is given in fig.2.3.

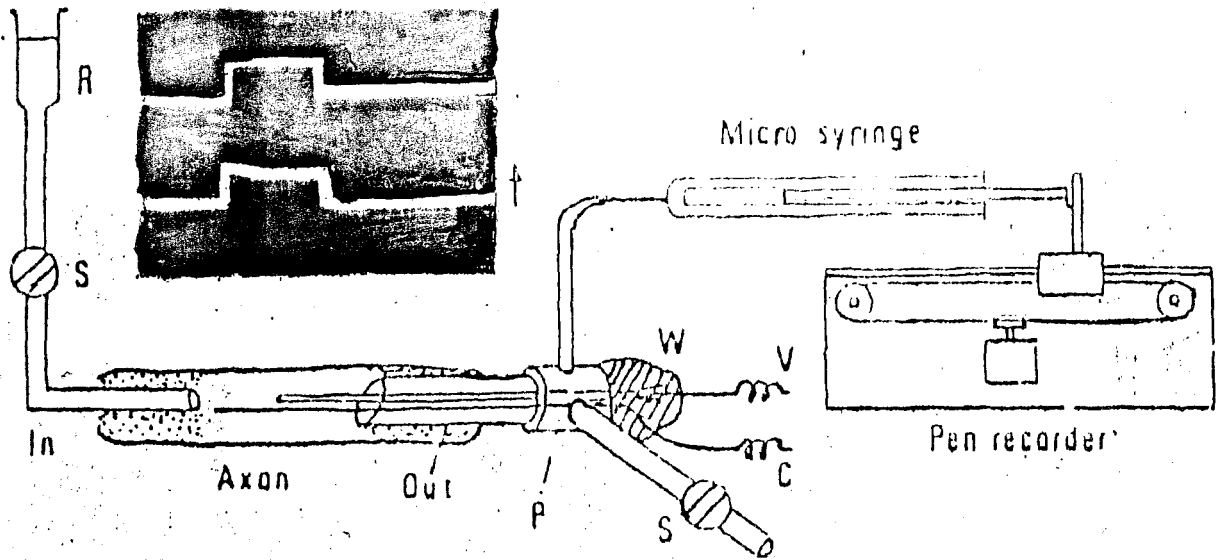


Fig.2.3 Schematic diagram of the experimental setup (not drawn to scale). IN,inlet pipette. OUT, outlet pipette. P,plexiglass tube. W,wax. S,stopcock. C,current electrode. V,potential electrode. R,reservoir of internal perfusion solution. INSET: An electrical pulse fed to pen recorder (upper trace) and a resultant change in diameter of axon (lower trace). A small piece of aluminum foil was placed on the axon and its movement was detected by an optical-fiber device. The arrow indicates a movement of the foil by $30\ \mu\text{m}$. The length of the perfusion zone was 5 mm, the diameter of axon $490\ \mu\text{m}$, the volume of the fluid injected into the axon $0,23\ \mu\text{l}$ and the duration of the pulse is 2 sec. (from Terakawa et al ,1982)

They estimated that the increase in surface area would be in the order of 5-10 per cent because of mechanical stimuli. As the diameters observed before and during the expansion of intracellular space did not change during a series of stimuli the

authors assumed that there was no leakage of internal solution.

The results of the experiment were as follows: After the stimuli applied, a hyperpolarization which grew quickly and decayed slowly on which a depolarizing response was superimposed was observed. The relation between stimulus amplitude and type was a sigmoidal hyperpolarizing one when the stimulus was an injection while the withdrawal of the same volume caused a small depolarization. If the latter stimulus magnitude was increased the response was again hyperpolarizing. The increase of external K^+ concentration at the expense of Na^+ caused a small depolarizing response. Application of TEA abolished the response by 65 per cent whereas application of $CoCl_2$, which is known to block Ca channels, externally caused irreversible suppression of the response. TTX, 4-Aminopyridine, neomycine, procaine, ethylalcohol, trypsin applied to the bathing medium or to the perfusion did not affect the response.

The discussion about the experiment made by the authors has revealed that by this type of mechanical stimuli the axonal membrane would be stretched in a circumferential direction which produces hyperpolarizing responses separated from depolarizing ones. Since TEA reduces the response magnitude and 4-Aminopyridine applied internally does not suppress it at all, the authors proposed that the observed response is resulted from the activation of leakage channels with a relatively high potassium selectivity for potassium ions.

2.4 Mechanosensitive Ion Channel

While making patch-clamp measurements of nicotinic ion channels on tissue cultered chick skeletal muscle Guharay & Sachs noticed an ion channel whose gating was dependent on suction applied to the pipette (Guharay F. et al, 1984). Investigation on this channel revealed that this stretch activated channel is poorly discriminating between Na and K ions. Depending on these findings the authors made an experiment in order to find out the properties of this channel. The experimental setup included the conventional patch-clamp technique (Hamill et al., 1983) as given in fig 2.4.1 where a micrometer driven syringe was used to apply suction. The tissue used in this experiment was the skeletal muscle cells of the above mentioned animal.

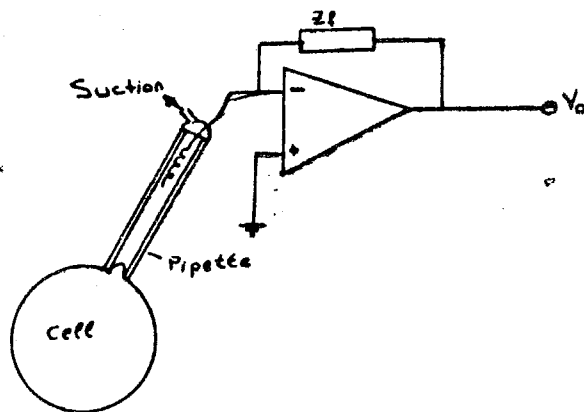
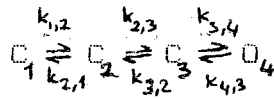


Fig.2.4.1. Schematic of the experimental setup using patch-clamp technique.

The followings are the results of this and of the proceeding experiment (Guharay F. et al, 1985): It is found that for this stretch activated channel, by employing Goldman's reversal

potential equation, the ion selectivity ratio between K and Na ions is calculated to be four. There was an insensitivity for Ca⁺⁺ rich mediums applied externally or internally and open time distributions could well fit into an exponential while close time distributions could only be fit into at least three exponentials. The effect of applied suction is a function of square of applied suction pressure to the third closed time constant. The cytochalasin which is known to destroy cytoskeletal structures increases this constant by a factor of 30. It was shown on the proceeding experiments made by the authors (Guharay F. et al, 1985) that this constant is also dependent on voltage and pH of the external solution. The kinetic model of this channel which was calculated by the authors is as follows;



where the only rate constant $k_{1,2}$ is both stretch, voltage and pH dependent as follows;

$$k_{1,2} = k_{1,2}^0 \exp(\alpha(\text{pH}) V + \beta(\text{pH}) F^2)$$

$$\alpha(\text{pH}) = 0.01 + 0.018 / (1 + 10^{(9.1 - \text{pH})})$$

$$\beta(\text{pH}) = 0.66 + 0.470 / (1 + 10^{(9.1 - \text{pH})})$$

The probability of channel being open was dependent on external K⁺ concentration.

The authors also discussed the possibility of conversion of deformation energy created by stretch to conformational changes occurring within the channel itself. With straightforward assumptions the authors resulted with a channel which gathers

deformation energy from an area of at least $3 \times 10^5 \text{ \AA}^2$ and as conductance and reversal potentials are not affected by pH the authors also concluded that the titrated site(s) are not close to mouth of channel. A schematic representation of this channel is given in fig.2.4.2.

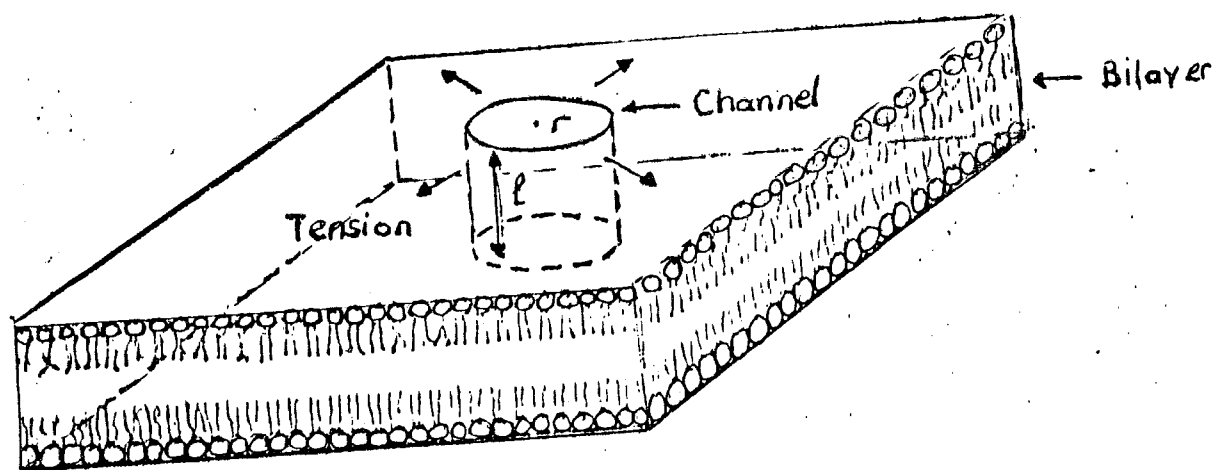


Fig.2.4.2 Schematic representation of the channel embedded in a lipid bilayer layer. The modelled channel is a cylindrical trans-membrane structure with a radius of "r" and length of "l". Isotropic tension in the membrane (shown by arrows) increases the channel radius, "r", and decreases its thickness, "l", assuming a constant volume, (from Guharay et al, 1984).

Although it seems complicated, one can summarize the above experimental findings and experimental setups as follows;

a. There is a difference between the responses because of short durational and long durational mechanical impulses delivered to the membrane of the experimental tissue. The former one causes rapid recovery while the latter one causes this recovery time to

elongate.

b. The stimulus amplitude is also responsible in the responses observed. There is a threshold of the stimulus amplitude determining the response of the membrane which can be either depolarization or generation of action potential.

c. The responses observed can be an hyperpolarization or depolarization because of the side on which the stimulus is applied.

d. The authors agree with the finding that the conductance increase observed can be of the leakage pathways. This result was supported by the experiments involving TTX and TEA which are known to block Na^+ and K^+ ion channels respectively.

e. An interesting observation was that on both experiments held by Terakawa et al & Guharay et al the response amplitude was highly dependent on external K^+ ion concentrations. At the same time CoCl_2 had an irreversible affect (former authors) and Ca^{++} ions had no influence on the responses (latter authors).

f. The mechanical pulses were delivered to the axon in the first two experiments by stylus which had diameters greater than the diameters of the axon while the latter two used differential pressures to induce the responses.

III. THE MODELS PROPOSED TO EXPLAIN THE PHENOMENA BY THE FORMER WORKERS

The mechanisms underlying the above mentioned phenomena are not well understood but most of the investigators working on the subject proposed that the ionic permeabilities associated with membrane potential are somehow reconstructed by the deformation of the membrane itself. But it is still in doubt whether the responses cited above are the major ones, which are the results of mechanical stimuli because, of the differences in the experimental methods and the tissue used. The attempts to express these findings as a general rule had the difficulties associated with the membrane models using the mechanical coefficients. Though a lot of data has been collected about these coefficients of red blood cells of different species and artificial bilayers, it is still a matter of debate as these data can be applied to excitable membranes of the same species because of the chemical composition differences between red blood cell and nervous tissue. An illustrative model of membrane of red blood cell is given in fig.3.1.1. Thus the attempts to resolve the effect of mechanical stimuli are generally using the ionic permeabilities and the cytoskeletons supporting the membranes mechanically in vivo and the properties of artificial membranes. Depending on these facts the solution of the problem of the transformation of deformation energy to activation energy of channel openings is not shared by the same authors.

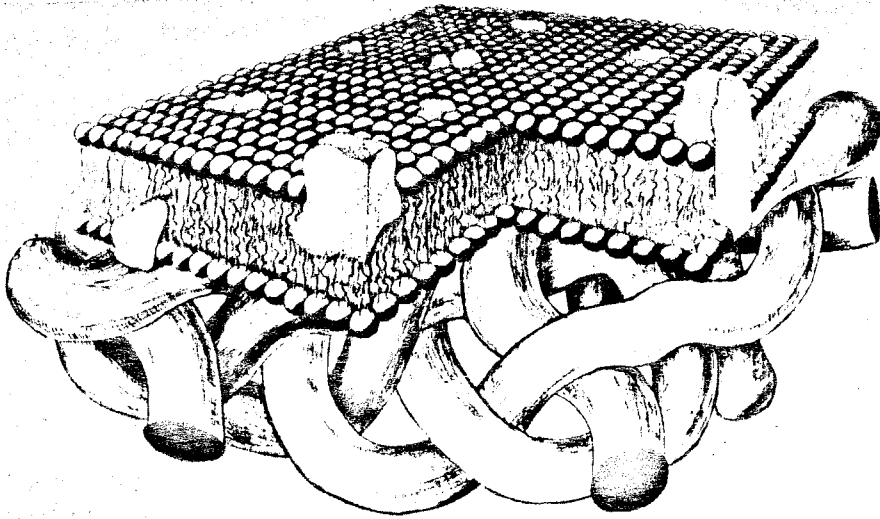


Fig. 3.1.1. An idealized view of the red blood cell membrane composite. (The underneath spectrin network provides structural rigidity and support for the fluid lipid-protein layer of the membrane.), (from Evans et al, 1980).

Taking into consideration of the problems above, the models proposed by different people to be cited here are:

3.1. The Transmembrane Macromolecule Rotation Model

In this model presented by Goto K. (1983) it is postulated that when acetylcholine combines with the acetylcholine receptor (AChR) subunit, hydrophobic subsites are exposed at the bound surface of AChR. Since hydrophobic portions are quite unstable, the subsites move to the center of the membrane, which is hydrophobic. It is postulated that the rotation of receptor subunits makes the center an ion channel, fig.3.1.2.

Ca^{++} flowing in through this ion channel causes the undercoating filaments to contract and this contraction results in the conduction of an action potential along the axon. The contraction of undercoating filaments induces transmembrane rotation of globular proteins connected to the filaments. At right angles to

the axon the force of hydrophobic bond between membrane

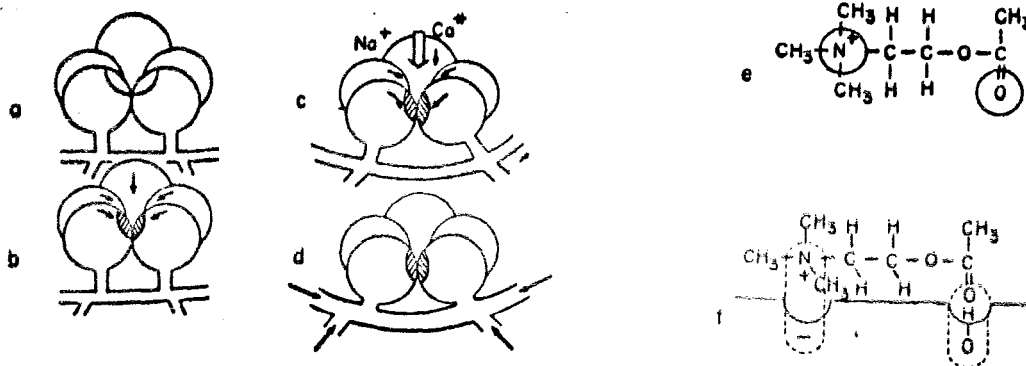


Fig. 3.1.2 Initiation of excitation. a: AChR in the resting stage. b: Binding of ACh to AChR. c: Formation of ion channel. d: Contraction of the underlying filaments by Ca^{++} influx. e: The structure of ACh. The subsite enclosed in a circle is hydrophilic. f: The ACh-bound surface of AChR becomes hydrophobic, (from Goto K., 1983).

macromolecules is so strong that many cylindrical lipid structures are formed. The gaps between the rotatory cylinders serve as ion channels. Ca^{++} passing through the ion channels allow for conduction of an action potential without attenuation, fig.3.1.3 and fig.3.1.4.

3.2. The Model Of Undercoat And Cytoskeletal Structures Which Supports Na^+ Channels

The experimental evidences for the basis of this model proposed by Matsumoto G. (1984a) were as follows:

a. Electron microscopic observation of the giant axon of the squid has revealed that axoplasmic microtubules are densely distributed near the inner surface of the axolemma and that they run

almost parallel with the longitudinal axis of the axon, forming

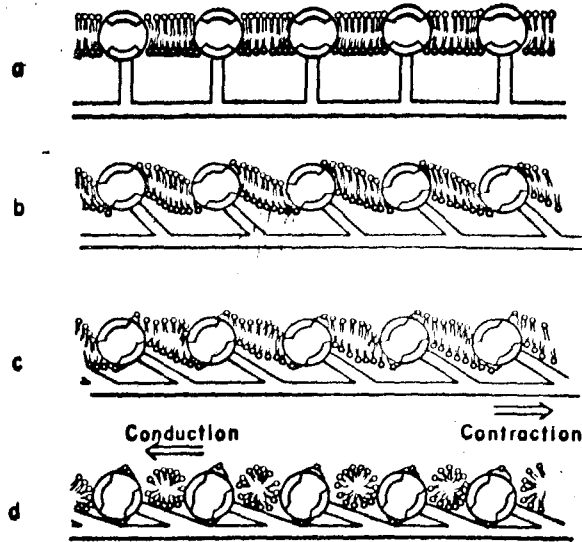


Fig. 3.1.3. Conduction of excitation. a: Axolemma in the resting state. b: Transmembrane rotation of protein molecules by contraction of undercoating filaments. c: Rotation of membrane macromolecules at a large angle. d: The cylinder formation, (from Goto K., 1983)

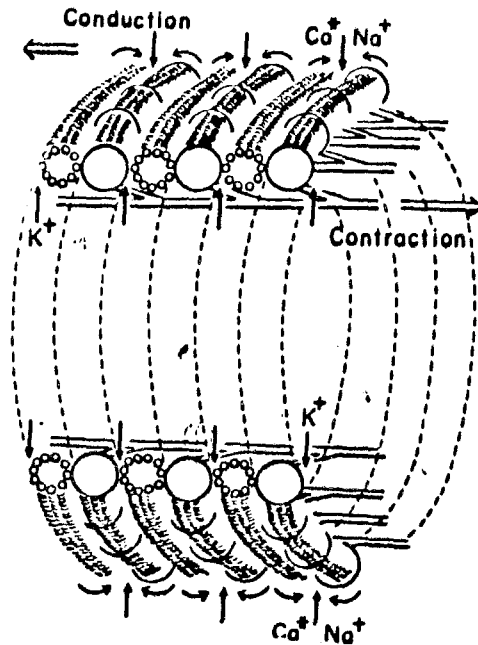


Fig. 3.1.4. The formation of the cylinders, (from Goto K., 1983).

cross-bridges and networks with neurofilaments and thin elements.

b. When microenvironments inside the squid giant axon were put into conditions suppressing microtubule assembly, by intracellularly perfusing the axon with a solution containing one of the reagents such as colchicine, vinblastine, podophyllotoxin, iodide and bromide, and polyanion of RNA, the sodium current was blocked in a concentration-dependent manner by the reagent while the potassium current was not much affected .

c. The membrane excitability of squid giant axons which had been deteriorated by internally perfusing with a solution containing colchicine or Ca^{++} ions could be restored by internally perfusing the axon with solution containing microtubule proteins and 260 K proteins (they are unique proteins located in the axoplasm underlying the excitable membrane in squid giant axons) under conditions favorable for microtubule assembly .

d. When the axon was intracellularly perfused with a solution containing a reagent supporting microtubule assembly such as Taxol or dimethyl sulfoxide (DMSO) (Matsumoto G., 1984b), entirely opposite effects upon sodium currents to those of the reagents suppressing the assembly were observed .

e. The effects of internal perfusion with a solution containing colchicine upon asymmetrical displacement currents were composed of two parts; colchicine-sensitive and colchicine-resistant. The colchicine-sensitive part was related to normal channels and has a definite rising phase while the colchicine-resistant one showed an instantaneous jump, followed by exponential decay .

In the proposed model of generating Na^{+} currents in squid giant axon it is assumed that Na^{+} channels proteins are embedded in the

lipid bilayer spatio-seperately from the voltage-sensitive proteins. The undercoat and cytoskeletal structures functionally connect both between the Na channel proteins and the voltage-sensitive protein and between the various Na channel proteins. The sodium channels open in the following time order. First, the voltage-receptor protein changes its conformation when the membrane is depolarized. Then, the information of the conformational change in the voltage receptor is transmitted to the gating subunit on the Na channel proteins through the undercoat and cytoskeletal structures, inducing the conformation of Na channel proteins to be in the open state.

Illustrative figures of the previous models and above mentioned model are given in Fig.3.2.1 and Fig.3.2.2.

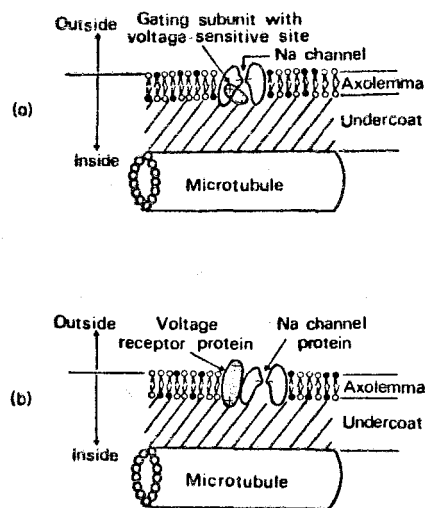


Fig. 3.2.1 A membrane model in which the axonal undercoat and cytoskeletal structures merely support the function of Na channels. a: the Na⁺ channel is a protein controlling ion-selective permeation with at least one gating subunit. b: The Na channel is constituted of two kinds of proteins neighbouring to each other; one is a voltage receptor protein and the other is a protein controlling ion-selective permeation, (from Matsumoto G., 1984a)

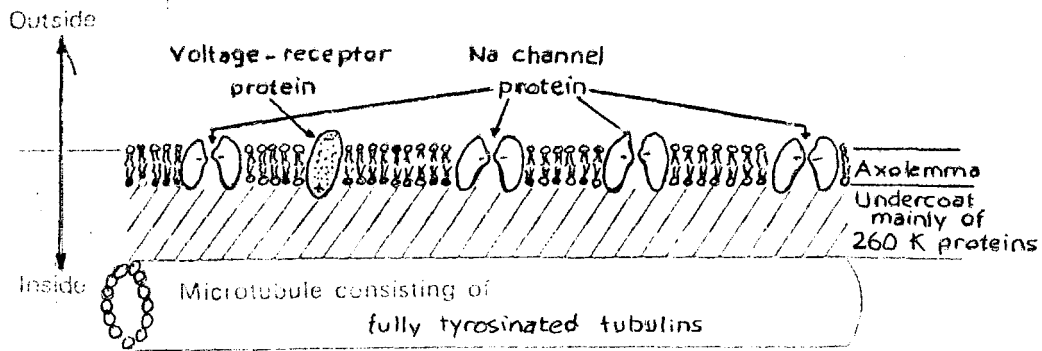


Fig. 3.2.2. A membrane model in which the axonal undercoat and cytoskeletal structures play a direct role in generating Na currents. The undercoat is constituted mainly of 260 K proteins and possibly of actins. Among cytoskeletal components of microtubules and neurofilaments, microtubules are essential in functioning Na channel, (from Matsumoto G., 1984a)

3.3 The Model Of Surface Charge Density Changes

In a simulated model (Gross D. et al, 1983) the authors discussed the possible role of changes in surface charge density resulting from stretch and proposed that the changes in the surface density would possibly change the intra-membraneous electrical field (see fig.3.3.1), thus opening trans-membrane ion conductance channels or reducing the ion selectivity of membrane via leak conductance pathways .

The effective membrane potential resulting from axon stretch will be as follows;

$$\Delta V_m \approx (\psi_e^\circ - \psi_a^\circ) \frac{\Delta l}{2l}$$

where ΔV_m is the change in membrane potential, ψ_e° is the inner surface potential, ψ_a° is the outer surface potential, and $\frac{\Delta l}{2l}$ is the strain occurred.

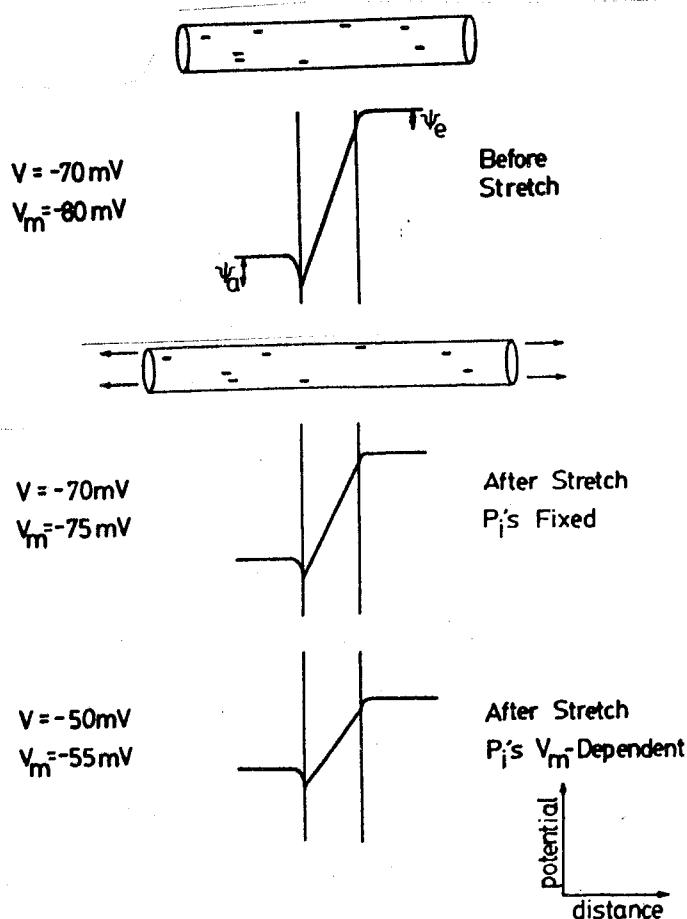


Fig. 3.3.1. The effect of axon stretch on surface potentials V_a and V_e , membrane potential V_m , and bulk to bulk potential V . (Top) Potential profiles for a hypothetical unstretch axon. (Middle) Potential profiles after stretch if ion permeabilities remain at their initial values. (Bottom) Potential profiles if permeabilities are allowed to adjust to the new V_m , (from Gross D. et al, 1983).

A plot of change in membrane potential vs. strain because of stretch using the equation above and assuming that the ionic permeabilities are allowed to adjust to the new V_m for different inner and outer surfaces is given in fig.3.3.2

On the other hand the authors discussed the possibility of simple mechanical deformation of ion channels and concluded that it was hard to believe such a possibility as it was difficult to imagine how there can be a mechanical linkage between channel proteins and lipid bilayer matrix.

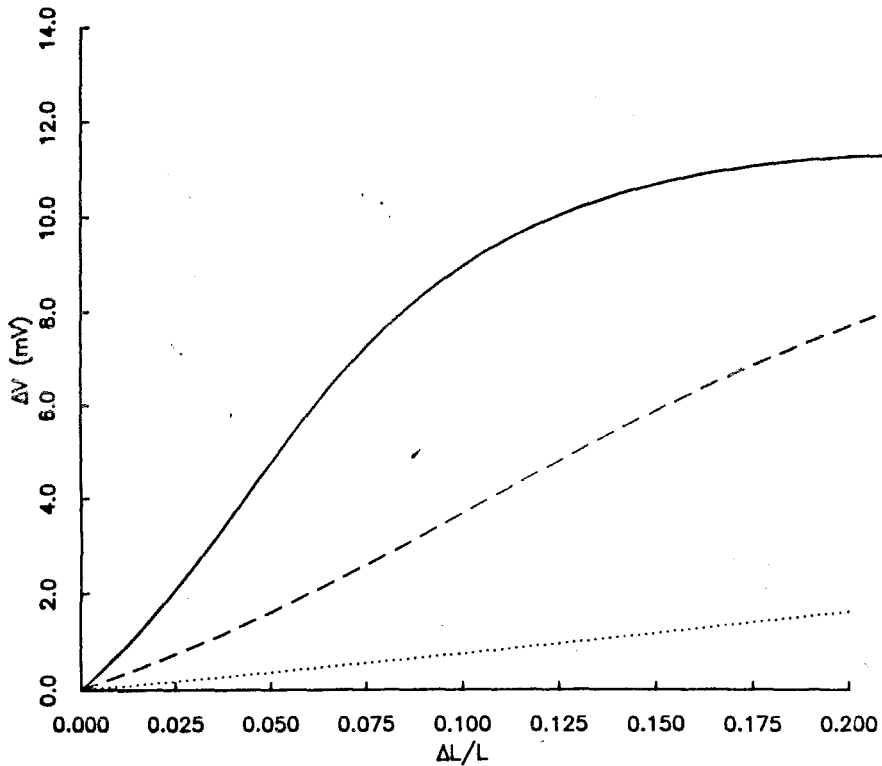


Fig. 3.3.2. Membrane depolarization vs axon stretch. (Solid) $\psi_e^o - \psi_a^o = 100$ mV, (dashed) $\psi_e^o - \psi_a^o = 40$ mV, (dotted) $\psi_e - \psi_a = 10$ mV, (from Gross D. et al, 1983).

3.4. The Model of Piezoelectric Effect Resulting from Mechanical Deformation

The model discussed by Guzelsu N. (1985) about piezoelectric effect resulting from striction of the biological membranes involves that as biological membranes are composed of polar lipids, any kind of pressure change upon it may cause a piezoelectric effect which could depolarize the membrane potential. On the other hand the author argued that, if the majority of polarization is associated with ion channels and other membrane proteins, and as it is assumed that piezoelectric proteins would be effectively mechanically decoupled from the

liquid-like lipid phase of the membrane because of large difference in elastic stiffness of the two phases, a piezoelectric deformation of the channels would be quite large which will cause ionic permeabilities to change.

BOĞAZIÇI ÜNİVERSİTESİ KÜTÜPHANASI

IV. THE PROPOSED MODEL WHICH SEEMS TO EXPLAIN THE PHENOMENA

In order to evaluate a membrane model to explain the mechanical sensitivities observed; first of all morphological features of different mechano-sensitive receptors, then the properties of these receptors must be taken into consideration.

4.1. Morphological Evidences

Studies in the past revealed that the morphological evidences are thought to be important by several investigators in physiological aspects. It is known that movement of stereocilia towards kinocilia results in depolarizing responses while withdrawal of stereocilia causes hyperpolarizing responses (Flock A.,1965), fig 4.1.1.

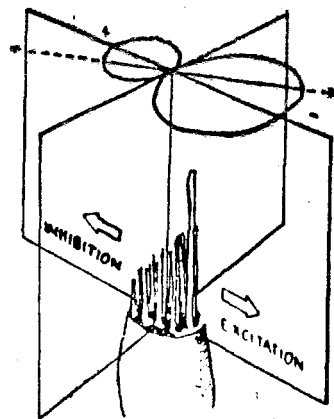


Fig. 4.1.1. Diagram illustrating the directional sensitivity of the hair cell (from Flock A.,1965).

The first attempts to resolve this directional sensitivity in terms of morphological aspects revealed that the hair process are anatomically polarized as shown in fig. 4.1.2a and fig. 4.1.2b (Lowenstein O. et al,1959).

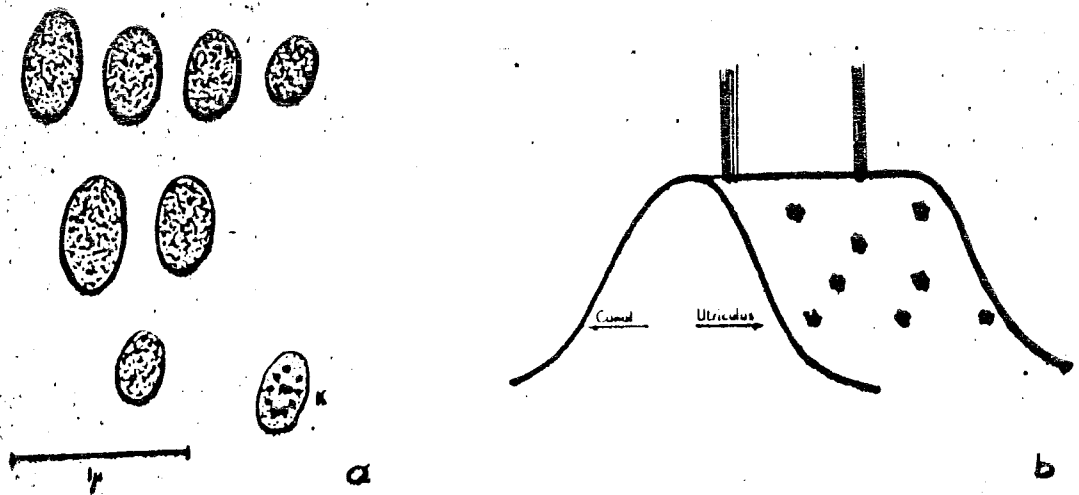


Fig. 4.1.2. a: Copy of an electron-photomicrograph of a slightly oblique section through part of a compound hair process from a sensory cell in the crista of a semi-circular canal. K, kinocilium. b: Diagrammatic representation of the crista of the horizontal semi-circular canal, showing two compound hairs and several compound hair bases on the side of crista facing the utriculus. Kinocilium is indicated in solid black. Note its spatial arrangement on the crista. Hairs and hair bases are magnified out of the proportion to the size of crista and their density is very much reduced. In a vertical canal the hair-bearing surface shown would face canalwards (from Lowenstein O. et al, 1959).

Later, when the morphological basis of this mechanical linkage was investigated (Hillman D.E. et al, 1971) it was found that kinocilium makes a plunging like action which produces a distension of the membrane on its base. Thus the authors postulated that this distension of the receptor membrane produces changes in ionic conductance which would lead to depolarization of the hair cell. Conversely a reduction in the amount of dimpling would decrease the depolarization, see fig. 4.1.3. This hypothesis was supported by the finding that there is a structural changes in auditory hairs during temporary deafness (Mulroy M.J. et al, 1984).

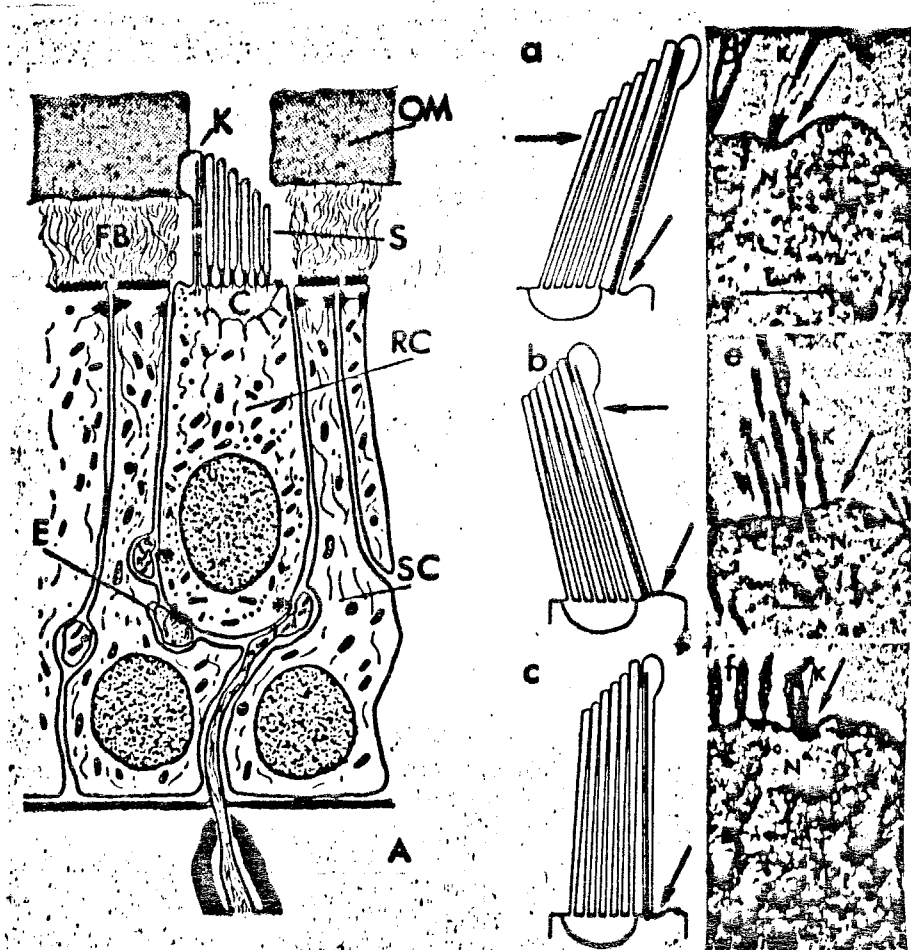


Fig. 4.1.3 (Left) Diagram shows the saccular epithelium with its receptor cell (RC) ciliary apparatus [kinocilium (K), stereocilia (S), cuticle (C)] and otolithic membrane (OM), and the filamentous base (FB) which supports the otoliths. (E) Efferent endings; (A) afferent ending. (Right) Diagrams and electron micrographs to show the effect of bending the cilia toward and away from the kinocilium. The relatively firm cuticular base (d,e, and f) and the attachment of the kinocilium to adjacent stereocilia (a,b, and c) causes the pliable receptor cell membrane in the region of the cuticular notch (N) to be thrust up or down with respect to the movements (a and d, and b and c). In the vertical position a slight dip is usually noted in both scanning and transmission electron microscopy (c and f). K, kinocilium; C, cuticle. (from Hillman D.E. et al, 1971). al, 1984).

On the other hand it was found that in Pacinian corpuscle there is a directional sensitivity where the receptor potential (depolarizing response) on compression generates hyperpolarizations in response to a gradually increasing compression after rotating them through 90 degrees along the long axis and vice versa (Ilyinsky D.B., 1965). The explanation of this findings were verified by regarding the geometry of the receptor and summarized as follows; When the mechanical stimuli were applied along the short axis of this cylinder (b) an increase in the ratio a/b (where a is the long axis) occurred, and consequently an increase in the surface area of the receptor membrane. On the other hand, the stimulus directed along the long axis (a) decreases the ratio and consequently the surface of the membrane (Nishi K. et al, 1968).

In response to mechanical stimulation of primary and secondary endings in isolated cat muscle spindle it is shown that the receptor potential per unit length change of spindle (gain) is constant up to a treshold displacement of 10 μm . With larger stretches the primary endings gain decreases as a power function of increasing displacement more steeply than the secondary endings (Hunt C.C. et al, 1980). This phenomena can also be attributed to the morphological and mechanical features of muscle spindle (Poppele F.E. et al, 1979).

The above mentioned morphological evidences implies that in receptor mechanisms structural properties are common to all to ensure a spatial distribution of tension on the membrane in the development of receptor potential.

4.2. The Properties of the Receptors

Several authors made experiments in order to find out the ionic properties of the receptors. They found out that if choline, an impermeable organic cation, replaces Na ions or procaine, which has a local anesthetic effect by decreasing both Na^+ and K^+ conductance, is added, the receptor potential decreases (Julian F.J. et al, 1962). On the other hand the permeabilities for various monovalent cations were $\text{Li}^+ > \text{Na}^+ > \text{K}^+ > \text{Rb}^+ > \text{Cs}^+ > \text{choline} > \text{TMA} > \text{TEA}$ while for divalent cations were $\text{Ca}^{++} > \text{Sr}^{++} > \text{Ba}^{++} > \text{Mn}^{++} > \text{Mg}^{++}$ (Ohmori H., 1985). TTX or TEA which selectively block normal Na and K channels respectively had no effect on the development of receptor potential (Loewenstein et al, 1963; Ganot et al, 1981; Terakawa et al, 1982) while Ca^{++} ions are indispensable (Ohmori H., 1985). Thus it seems plausible that the ionic permeabilities associated with these findings are different than the normal excitation of excitable membrane.

4.3. The Possible Models

Depending on the events above one may propose the possible models responsible for the generation of receptor potential as follows;

4.3.1. Piezoelectric Effect

As described above piezoelectric effect may have an importance but as seen from the ionic evidences such a possibility can be ignored because of the CoCl_2 and Ca^{++} antagonism and of the essential Ca ion concentration cannot be explained by this model. But

one may assume that these chemicals can alter the piezoelectric coefficients which in turn causes the observed result. Hence, before having more knowledge about the molecular level structures of membranes this possibility is left in question.

4.3.2. The Effect of Streaming Potential

This model can also be ignored because it is shown on squid giant axon that; the water flow facilitates an ionic flow through the potassium channel in the same direction and suppresses the ionic flow in the opposite direction resulting a hyperpolarization (Kukita F. et al, 1975) which is in contrast with the observed findings. It is a possibility that the results of Terakawa S. et al is consistent with this model since, although the authors assumed that there was no leakage of internal perfusion fluid, close inspection of the experimental data about the change in membrane diameter reveals either an outward water flow or the relaxation of the membrane.

4.3.3. The Changes in Surface Charge Density

This model has the deficiencies in explaining the TTX and TEA insensitivities while the predicted amount of depolarization was not enough to elongate the open time durations of Na^+ channels. But one may argue that stretch causes opening of Na^+ channels different than normal TTX sensitive ones. The results of their simulation showed that in order to obtain a depolarization of 15 mV a distension of 15 per cent is needed, on the other hand it was shown that a distension of two or three per cent causes the

membrane to rupture (Evans E.A. et al,1980).

4.3.4. Specific Mechanoelectric Transduction Channel

The ion channel proposed by Guharay et al seems to explain the phenomena well. But in the evaluation of model the authors assumed that the deformation energy resulting from stretch is gathered from all the hemisphere. Instead it was shown that the calculated deformation is not only on the hemisphere but also on the cylinder formed inside the patch and on the membrane outside the patch.pipette (Evans E.A. et al,1980). Thus the calculation made on this assumption is invalid which gives a channel diameter smaller than it should be. Apart from this the authors assumed a single ion channel which was embedded in the bilayer which seems plausible because there were no direct evidence for this channel to be single. Even if it was so the strain developed inside the hemisphere was not isotropic but instead it is cylindrical which results in a cylindrical distribution of tension (see fig. 4.3.4.1). The value evaluated from proposed data the authors resulted from a channel density of $0.16 / \mu\text{m}^2$ which seems relatively small to contribute such a value of depolarization resulting from stretch. Although the authors employed a cytoskeletal network as in red blood cell membrane to avoid from such a big protein, in the order of 16 MD which should be observed before, to explain the gating of this channel, it is also in debate how this channel protein can undergo a conformational change by the mechanical linkage between the protein and the cytoskeletal network.

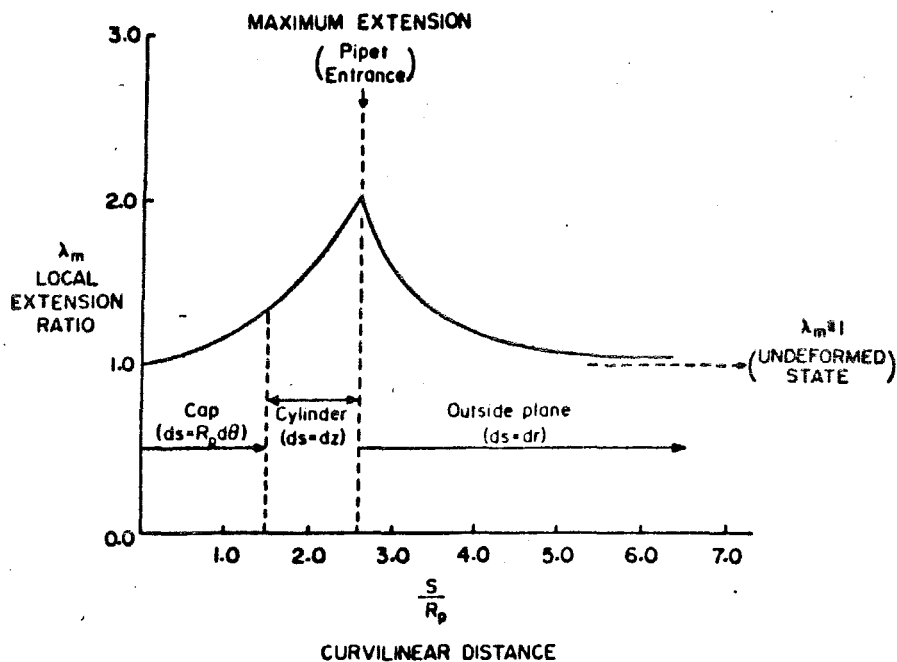


Fig. 4.3.4.1 Nonuniform extension produced by micropipet aspiration of a surface at a constant area. The extension ratio is plotted as a function of curvilinear distance, s , along the meridian from the pole of the spheroidal cap to the outer surface of membrane, (from Evans E.A. et al, 1980).

4.3.5. Transmembrane Macromolecule Rotation Model

The author suggested that the rotation of transmembrane macromolecules may form unstable cylindrical lipids which serve as ion channels. Although the contraction cytoskeletal fibers which may be composed of actin and myosin filaments seems likely, the rotation of macromolecules are dependent on flip flop rate of excitable membrane. Current data indicates that this rate is in the order of 10 or 30 days for half life (Harrison R. et al, 1980). Therefore the assumption of rotation is inconsistent in the light of the above cited rate. Even if it was so, because the model proposes cylindrical formation which are perpendicular to the longitudinal axis of axon, the model seems unsatisfactory in explaining why the stability of membrane is preserved after a few

excitation and in explaining why to occur such a preferred formation.

4.4. The Proposed Model of Lipid Rupture

4.4.1. Basis of the Model

The above scheme suggests that in order to propose a hypothetical membrane model which seems to explain the mechano-electrical transduction process;

a. The response dependence to the stimulus amplitude must be satisfied.

b. Directional sensitivity of the membrane should be considered.

c. The difference in responses between short and long durational stimuli is to be regarded.

d. TTX and TEA insensitivity must be explained which implies that normal ionic channels are not involved in the process.

e. The indispensibility of internal Ca^{++} ions must be preserved.

f. The underlying network which seems to have an importance in generating the responses must be related to the model proposed.

g. The effect of cytochalasin, which destroys intracellular network, in increasing the mechanical sensitivity should also be considered.

h. If an ionic channel is involved in the process it must have a poor discrimination between Na^+ and K^+ ions.

The model which seems to satisfy the above conditions more likely is : Assuming the biological membrane looks alike to the membrane structure given in Fig. 3.1.1, it is evident that the membrane material properties can only be considered as a conti-

num in the two dimensions, which describe the membrane surface. In the third dimension, thickness, the membrane exhibits molecular structure and discontinuity that preclude treatment as a continuous material in this direction. Consequently membrane is appropriately represented as a two-dimensional continua with possible isotropy in the surface plane. Therefore surface properties represent the effects integrated over the composite molecular structure in the thickness dimension. Since the lipids are in a fluid state, solid characteristics of the membrane must be attributed to connections of proteins and other molecules associated with the membrane. In Fig.3.1.1. the spectrin network is shown as providing structural rigidity and support for the fluid component of the membrane and is often referred as cytoskeleton. A variety of additional structures may exist in association with the cell membrane, e.g., connective tissue, cytoplasmic elements, microtubules, etc. These can also provide structural rigidity and even active deformation.

4.4.2 The Model

Assuming a mechanical force in the form of stretch is applied to the membrane in surface plane, it can be considered that the stress occurred must be balanced with the intramolecular forces of lipids and the deformation reactance of spectrin-protein network. If another assumption is made by implementing that the cytoskeletal network provides the main counter acting forces with respect to lipid structures, it can be speculated that if the viscoelastic forces between lipid-lipid interaction is greater than the lipid-protein interaction the strain occurred because of

stress between molecular elements would be expected to occur more likely at the lipid-protein interface. This displacement will be diminished by the reformation of the membrane. But from the second assumption it is evident that because of the deformation time constant, the unstable gap between the protein lipid interface can serve as an ion channel. A schematic representation of response initiation resulting from mechanical stimulus due to presented model is given in fig.4.4.2.

4.4.3 Discussion of the Model

The evidences supporting the above assumptions can be given as follows:

- a. E.s.r., n.m.r. and, more recently, fluorescence techniques have all been applied to measure the lateral diffusion coefficients (D) of lipid probes, and similar values of D (of the order of 10^{-8} cm^2/sec) have been found in a range of cell membranes and, above the phase transition, in model phospholipid bilayer systems.
- b. The lateral diffusion of protein molecules in a number of cell membranes has been examined by a variety of methods and has been found to be generally slower ($D=10^{-11}$ - 10^{-9} cm^2/sec) than that of lipids.
- c. The proteins do not interact with the bulk of the lipid component, in some cases they may interact with specific lipids, presumably those adjacent to them. It has been reported that such a tightly bound lipid in the protein complex cytochrome oxidase of mitochondrial membranes (Singer S.J., 1975) exists.
- d. Different methods applied to resolve viscoelastic character-

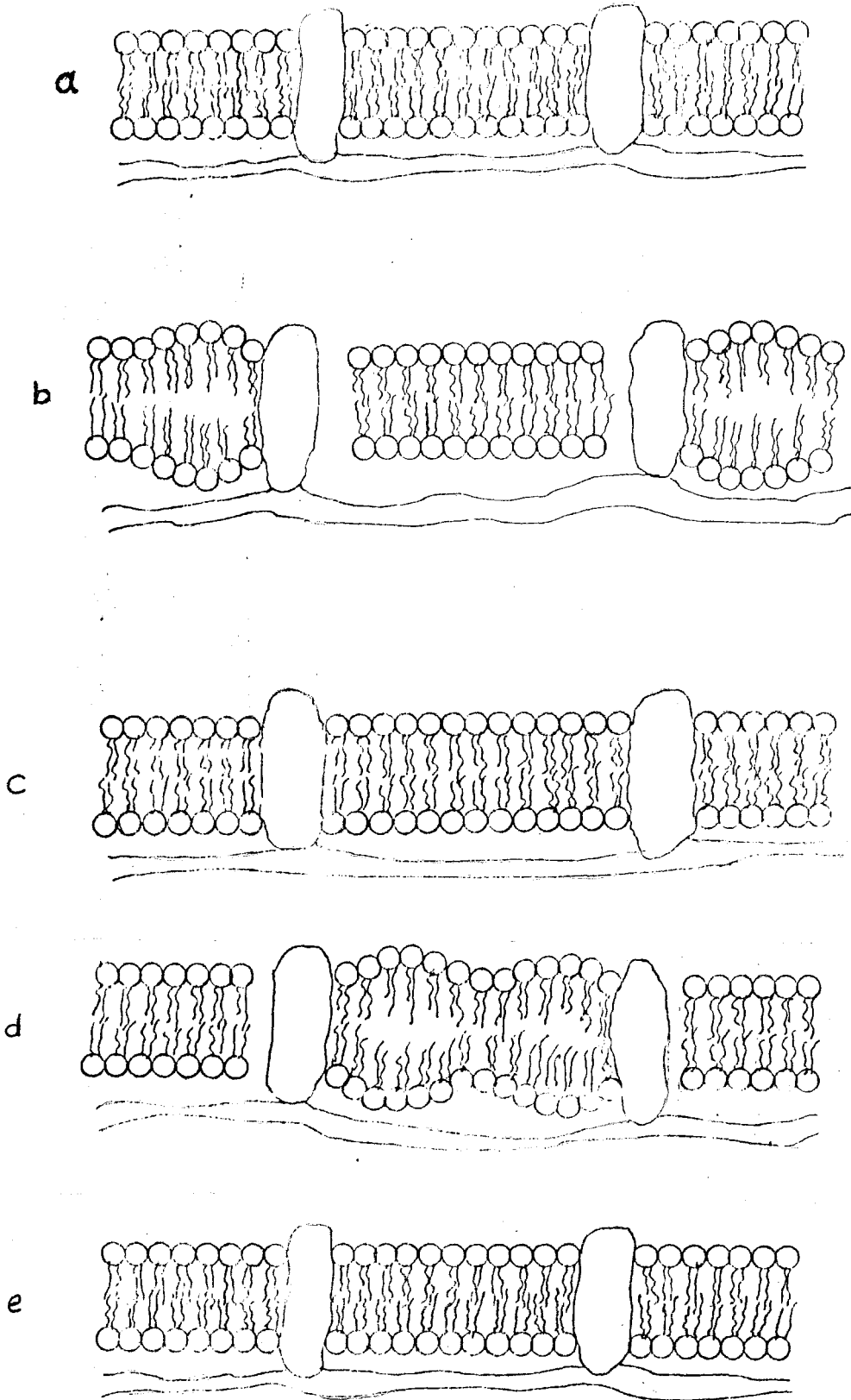


Fig.4.4.2. a. Resting state. b. Stretch of the membrane ,formation of channels. c. Reformation of membrane. d. Release of stretch, formation of channels. e. Turning to initial conditions. Note the expected displacement of the membrane surface.

istics of erythrocyte membrane revealed that this parameter is of the order of 10^3 dyn-sec/cm, while experiments held on artificial phospholipid membrane gives a coefficient of 250 - 17 dyn-sec/cm (Snik A.F.M. et al,1982).

e. It has been reported that the osmotic swelling of erythrocyte results in leakage of cations and hemoglobin (Hoffman J.F.,1975).

Therefore the model proposed seems to explain phenomena well because it also satisfies the conditions 4.4.1 a - h. For example, the response amplitude must be relevant to the response amplitude since the ionic pore diameter would increase on increase of the stress while the number of such formations are expected to increase also. On the other hand, as the obtained pore is nonspecific and different from the normal channel proteins it also explains the insensitivities for TTX and TEA, while it shows no discriminations between K^+ and Na^+ ions. Ca^{++} ion indispensibility is also preserved in the model since its known that the actin-myosin complexes are sensitive to Ca^{++} by contracting, thus stiffening the membrane, while from the second assumption it is important to note that the cytoskeletal structures mainly support the membrane. The sensitivity increasing effect of cytochalasin can be attributed to its destroying effect on cytoskeletal network and causing membrane to be less tough and easily deformable. The effect of $CoCl_2$ which is irreversable can be understandable since the blocking effect of Co^{++} on Ca^{++} channels is well defined. The membrane sensitivity because of stretch site can be explained by the difference in intracellular and extracellular network. It was reported that the anchoring nodes of membrane proteins are mainly intracellularly

which implies that the stress to be overcome by the cytoskeletal network are in the form of pressure upon restriction of the membrane area and vica versa.

4.4.4. Predictions of the Model

a. The model involves two time constants which are appearing from the phase difference of the lipid-lipid and of the protein-lipid structures. One of it appears from the time-lag of proteins to move in the lipid bilayer while the other comes from the reformation of lipid bilayer by readjusting the minimum entropy conditions. Thus there should be evidences demonstrating the two time constants which appears on the beginning and on the removal of the stretch while the other in the sustaining and postend period of the stimulus.

b. Another prediction is that there must be a difference in amplitude to obtain similar responses between delivering stimulus to the membrane surface spatially or locally. The former one would need greater amplitude while the latter would need smaller amplitude.

c. There should also exist a propagation of response beginning from a preferred region, if the considered surface is not large enough to ignore the changes in membrane elements since the initial assumption was the isotropy of membrane in two dimensions (surface plane). The anisotropy of the material properties in microscopic areas would lead an uneven distribution of strain which inturn cause the response to initiate from a preferred region.

d. The model involves a small displacement to occur on the surface of the membrane in the order of a few ten nanometers when the mechanical stimulus is delivered because of the striction of lipid bilayer on the opposite direction of pore formation. This displacement will be diminished by the reformation of the membrane. Recently it has been shown that such a displacement to occur in different excitable membranes of different species (Tasaki I., et al 1980a, 1980b & 1982).

V. THE EXPERIMENTAL SETUP DESIGNED TO TEST THE MODEL

5.1 Selection of the Experimental Protocol

5.1.1 Selection of the Material

The tissue that will be used in the experiments should be well defined in physiological aspects so that a direct comparison of the evaluated data can easily be made. The literature on this subject shows that the general material used is either Squid giant axon or Myxicola giant axon for being easy to prepare and for having relatively large diameters for application of internal electrodes. Thus the data relevant to their physiological properties and to their responses to different chemicals can easily be obtained elsewhere (Binstock L. et al 1967, Binstock L. et al 1969, Ganot G. et al 1981, Hodgkin A.L. et al 1952, Julian F.J. et al 1962, Terekawa S. et al 1982 and Kukita F. et al 1983). As it seems impossible to obtain Myxicola preparations in Turkey, the selection of animal was restricted and therefore it was found out that Turkish squids named commercially "Kalamar" and "Murrekep baligi" satisfies the anatomical and physiological conditions. The attempts to use the giant nerve of earthworm were faced with, although there are some papers mentioning about the properties of this nerve, the nerve was insuitable for experimental procedures (see below) for being small in diameter. Another attempt to use the very large membrane of chicken egg-yolk membrane was unsuccessful because of the rapid variations in its resting membrane potential.

5.1.2. Selection of Method to Deliver the Mechanical Stimulus

The mechanical pulses can be delivered to the membrane by pressing the membrane by a stylus, by stretching the axon longitudinally or applying pressure differences spatially or locally. Since there are problems associated with the reconstruction of deformation distribution of a cylindrical membrane which can be modelled as a giant axon of a species and to introduce mechanical pulses when there is intracellular electrodes, the problems are relatively simplified when the membrane is dissected to form a planar surface. It was reported that this form of membrane also exhibits the same physiological responses with the cylindrical membranes (Llano I. et al 1984). The mechanical stimulus then can be delivered to the membrane by the help of a polyethylene stylus. The restrictions associated with the mechanical design of the fixation of membrane caused to select giant axons having diameters greater than 500 μm .

The stimulus type and the site of application (intra- or extracellularly) is to be considered to resolve the above mentioned predictions of the proposed model. Therefore the stimulus is delivered by a stepper-motor driven micrometer in a stepwise manner.

5.1.3. Selection of the Recording System

Since the responses characteristics to be measured are not well known because of the different data published elsewhere and the experimental protocol is highly different from the above cited methods with respect to the membrane assembly, the design and

implementation of a flexible recording system was taken into consideration.

5.1.4. Selection of Perfusion Solutions

As the preparation procedure is relatively simple and changes of the membrane properties are quite well known, the mediums in which the planar membrane will be immersed are prepared conventionally. The relevant data about the effect of different chemicals when applied intra- or extracellularly are described elsewhere, (Baker P.F., et al 1962a).

5.2. The Experimental Methods

The general setup to deliver and to collect the data is illustrated in fig 5.2.

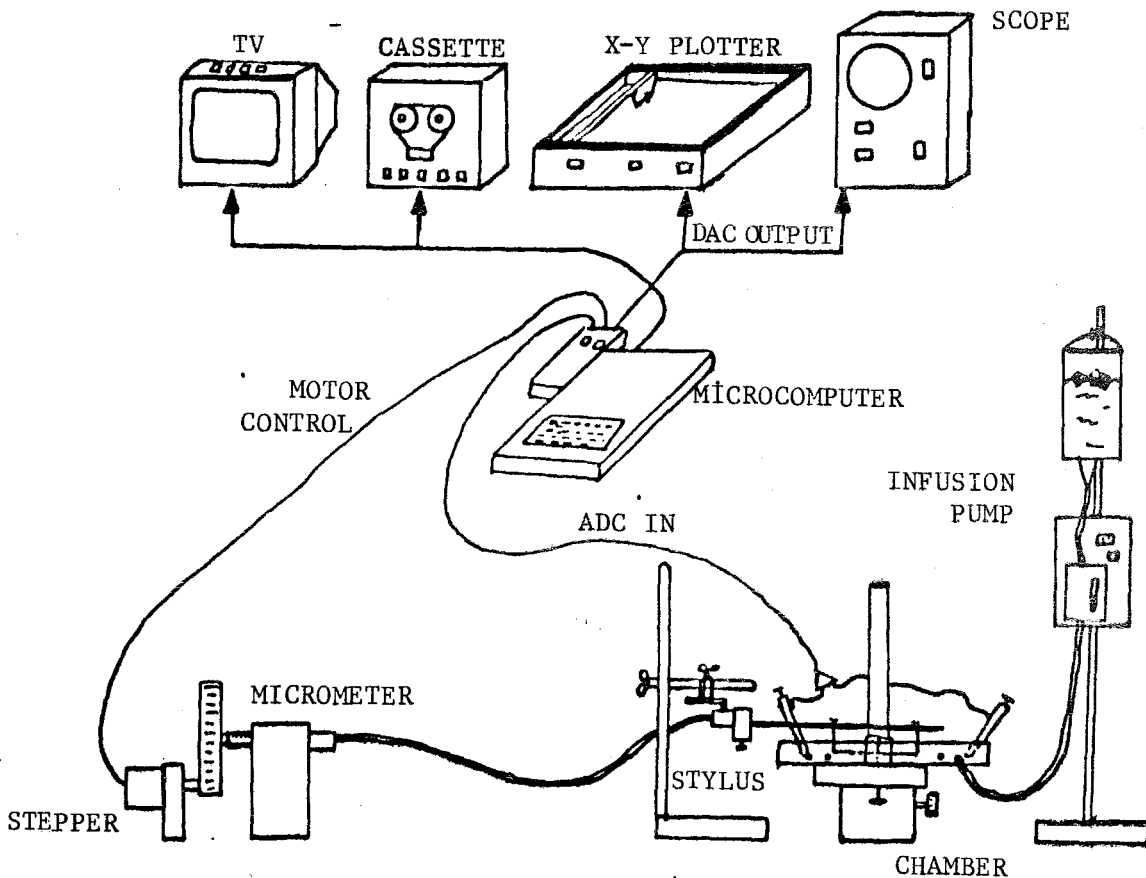


Fig.5.2. Experimental arrangement.

5.2.1. Preparation Of The Membrane

Giant nerves of squid are found in the mantle of squid. The suitable giant nerves of squid can be found when the mantle is dissected ventrally. The stellar ganglia in which the axons will appear, lie on each side of the mantle close to the ink duct of the squid. The peripheral distribution of the third-order giants follows the stellar nerves. These are easily seen in life in the translucent mantle muscle with favorable illumination. The zone of muscle supplied and the length and diameter of the axon are relatively small for the anteriormost and largest for the last stellar nerve which is commonly called "the" giant fiber of "the" squid. The largest diameters reach 940 μm in *Loligo Forbesi*, 750 μm in *L. Pealii*. Fine branches begin fairly close to the stellate ganglion and bifurcations somewhat farther away. For an anatomical description see Appendix A. After dissecting the axon from one end, a cannula filled with perfusion fluid is tied into the distal end. The axon is placed on a rubber pad and the axoplasm is extruded by passing a rubber-covered roller over it in a series of sweeps (fig. 5.2.1.1). At the end of this operation after immersing the axon in sea water the remaining piece of axoplasm near cannula is moved out by the flow of perfusion fluid which is about 6 $\mu\text{l}/\text{min}$ (fig 5.2.1.2). When the perfusion fluid flows out from the other end of axon, another cannula is tied into this end also.

5.2.2. Membrane Fixation Techniques

Under a dissection microscope the cylindrical membrane of axon cut-open by fine blades and then it is fixed on the mechanical

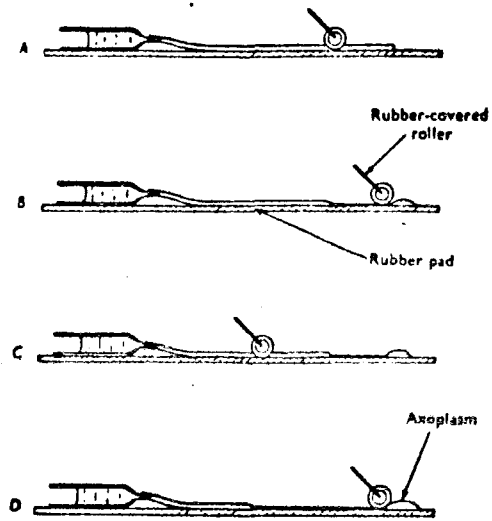


Fig.5.2.1.1 Extrusion of axoplasm

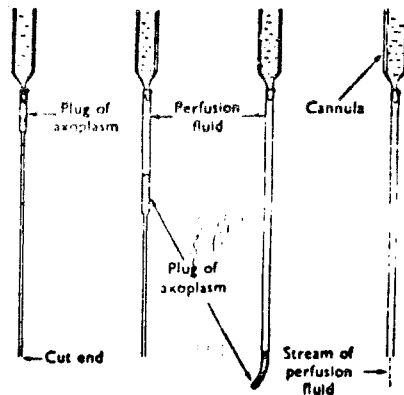


Fig.5.2.1.2 Re-inflation of extruded axon with perfusion fluid.

fixation table. The manufacturing information of the table is given in Appendix B. To improve the electrical and chemical insulation of either side of the membrane, the table is coated with fine layer of vaseline oil. The table which was assembled is then moved to a two chambered specimen holder (see Appendix B for manufacturing details) where it will serve as an insulator between the two chambers of extra- & intra-cellular fluids. The gap between the chambers is adjusted so that, when the table coated with vaseline is pushed in, a full insulation may occur, In order to have a temperature controlled environment each chamber includes two glass pipettes passing through the chamber. The ice cold water pumped at a specific rate by an infusion pump sustains the cooling of the chamber solutions.

5.2.3. Composition of the Solutions

The artificial sea water consists of (in meq. ions/lt) 10 K^+ , 526 Na^+ , 50 Ca^{++} , 633 Cl^- , 2.5 H CO_3^- while internal solution's composition is 610 K^+ , 560 Cl^- , 30 $H_2PO_4^-$ and the pH is adjusted to about 7.7 adding by KOH to KH_2PO_4 in final solution.

5.2.4 Preparation of Pipettes

Silver wires of 0.1 mm diameter and 15 cm long were immersed in an electrolyte consisting of 3 M KCl as an anode while a carbon rod served as a cathode. The rectangular pulses of 30 mA amplitude an 20 seconds duration is applied to the electrodes. After the first delivery of pulse the polarity is changed to eliminate the Cl deposition on the anode. This protocol is continued until a black film of $AgCl_3$ appeared on the surface of

silver wire. The other ends are coated with solder to have a good contact with long copper wire electrode. The agar-agar is heated with 3 M KCl and sucked inside a syringe in which the coiled Ag-AgCl₃ electrode is immersed. After cooling this assembly the tips of electrodes are immersed in a beaker containing 3 M KCl to avoid drying.

5.2.5. Data Acquisition

The membrane potential of axon is amplified in the first stage by a variable gain differential amplifier which has a bandwidth of 3560 Hz and a CMMR of ≥ 60 dB. Because of the offset problems associated with the Analog to Digital Converter (ADC) which has an operation range between 0-5 Volts, the amplified signal is then added by a variable voltage to fall in this region. The ADC is an eight bit converter which has a conversion time of 100 μ sec. The 8 bit parallel data is then fed to a R6502 based microcomputer to be stored and evaluated. The block and printed circuit diagrams of data translation are given in Appendix C.

5.2.7. Control of Mechanical Pulse Sequence and Data Acquisition

The control and data collection is done by the master program in Appendix D which uses co-programs given in Appendix E. The algorithm of the master program is given in fig 5.2.7.

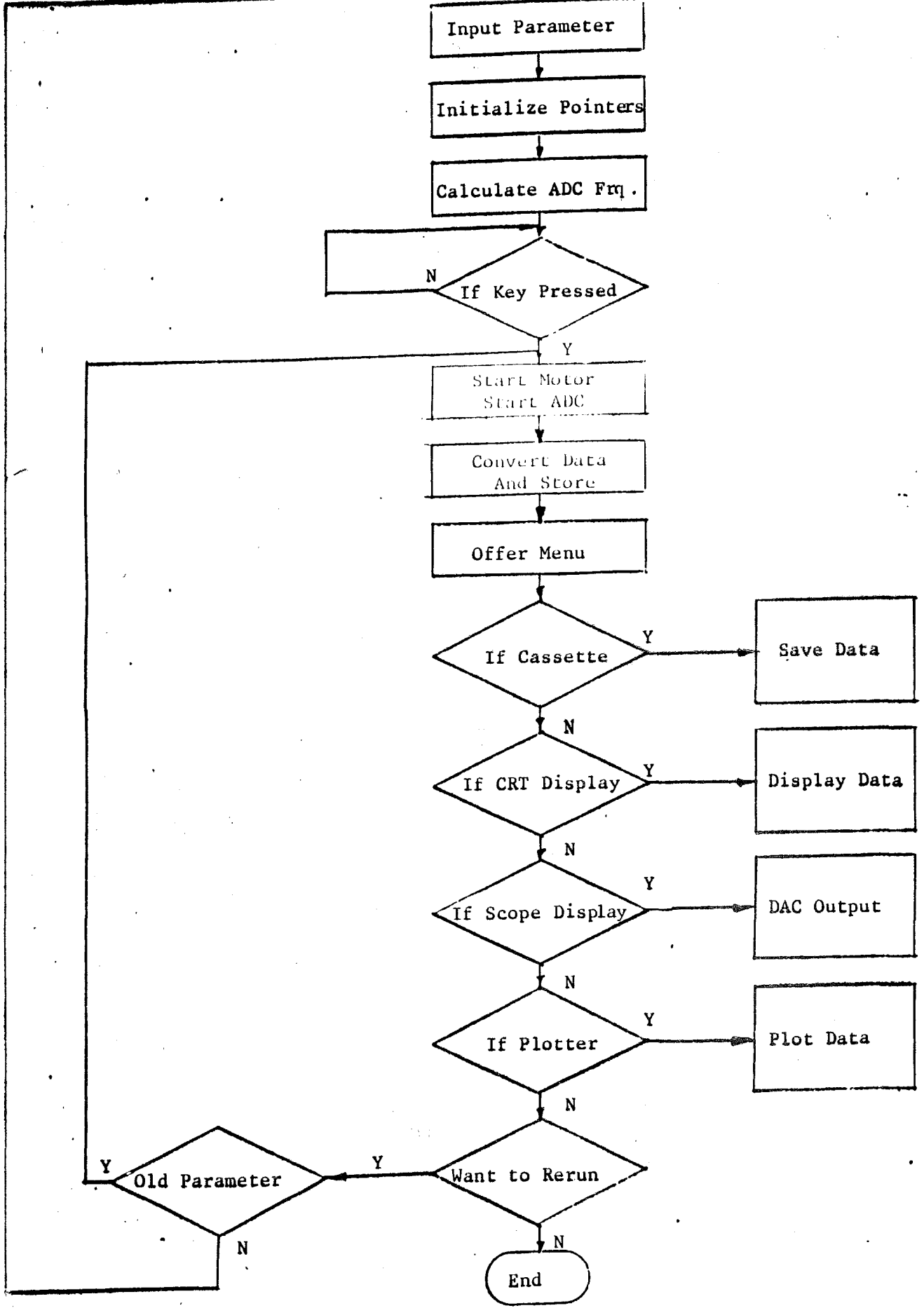


Fig.5.2.7. Algorithm for the Master program.

VI. CRITIQUE OF THE METHOD

It can be shown that the extension produced by impulse is proportional to the impulse amplitude. Assuming the membrane as an isotropic and elastic materials the outlines of this calculation is given in Appendix F. Since it is so, by changing the stimulus amplitude one can consider that the displacements occurred in macroscopic level is varied in a linear manner. Application of step-type variations in the stimulus amplitude can show the predicted time constants. If a pre-stretched condition is achieved, the changes to be observed in response amplitude will show the participations of cytoskeletal structures in generating of counter acting forces. The application of stimulus either inwards or outwards is expected to show the site of responsible protein anchoring points. By changing the stylus diameter it is possible to evaluate the second prediction of the model which implies that upon application of spatial deformation, in order to observe the same response amplitude, the amplitude of impulse must be increased. Since the bandwidth of the amplifier system is restricted it may not be possible to observe the first order time constants for these constants are expected to be small enough. However application of sinusoidal type of excitation may be able to show this time constant if a phase difference between the impulse and response is observed. But this time there will be a problem arising from the conversion cycle since the maximum conversion frequency is 3 KHz because of the time limits of the

CPU. This problem could be solved by using a very efficient program but it was shown that there is a problem related with such modifications made on the software controlled ADC (Lenz J.E. et al,1985). The problem arises from the execution of system bus using noisy instructions at critical sample and hold times. Thus in the software configured it was taken into consideration but this inturn caused a decrease in the efficiency of the program. The ionic currents responsible for the expected changes in the membrane potentials can also be evaluated by this method and needs further research.

APPENDIX A

ANATOMICAL DESCRIPTION OF THE GIANT FIBER OF THE SQUID

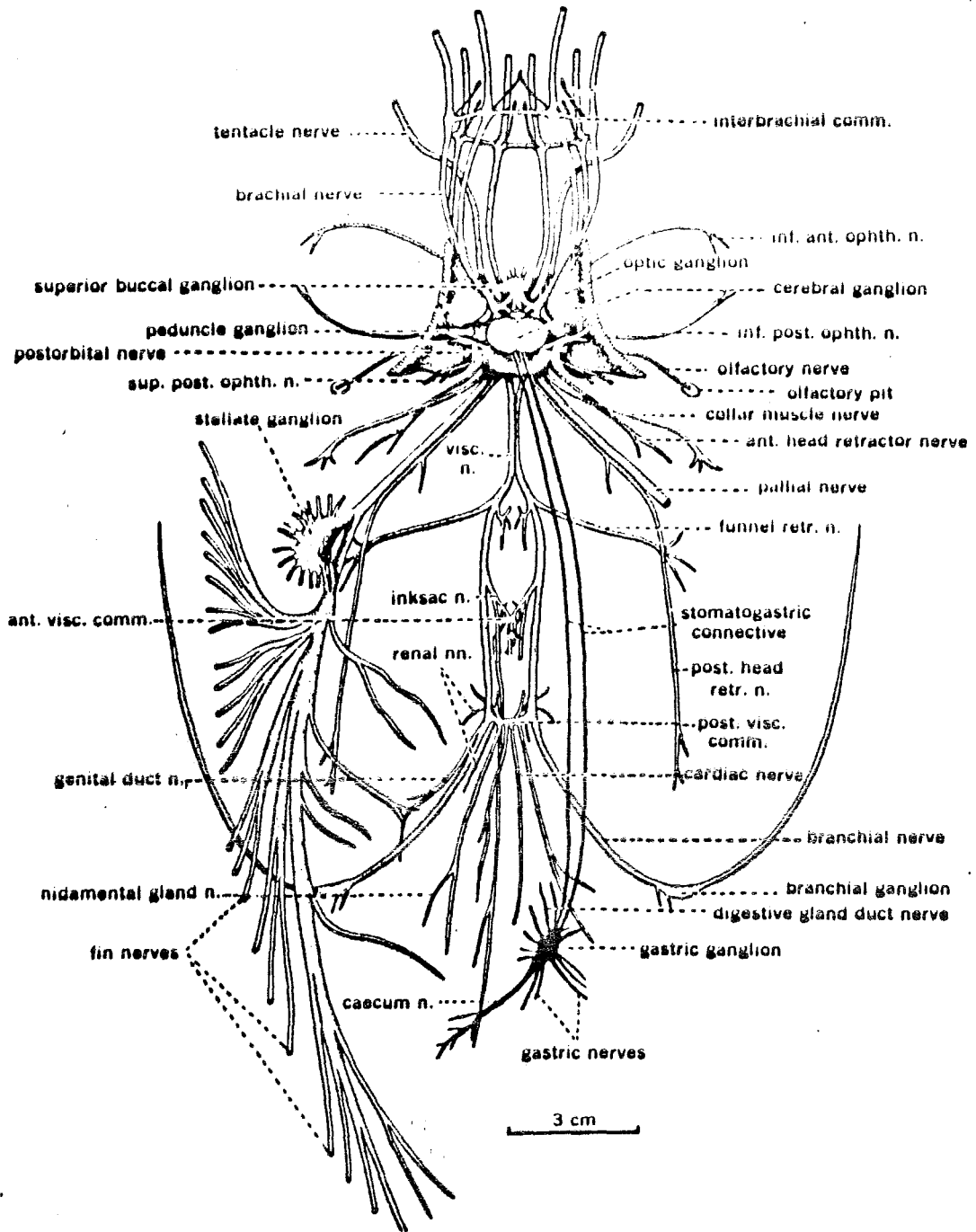


Fig.A.1. Nervous system of *Sepia*, dorsal view. Right stellate ganglion and fin nerves omitted; Stomatogastric system in black. ant., anterior; comm., commisure; inf. ant.(post.) ophth. n., inferior anterior (posterior) ophthalmic nerve; n.,nerve; post., posterior; retr., retractor; sup.post.ophth.n.,superior posterior ophthalmic nerve; visc.,visceral, (from Bullock T.H. et al,1965)

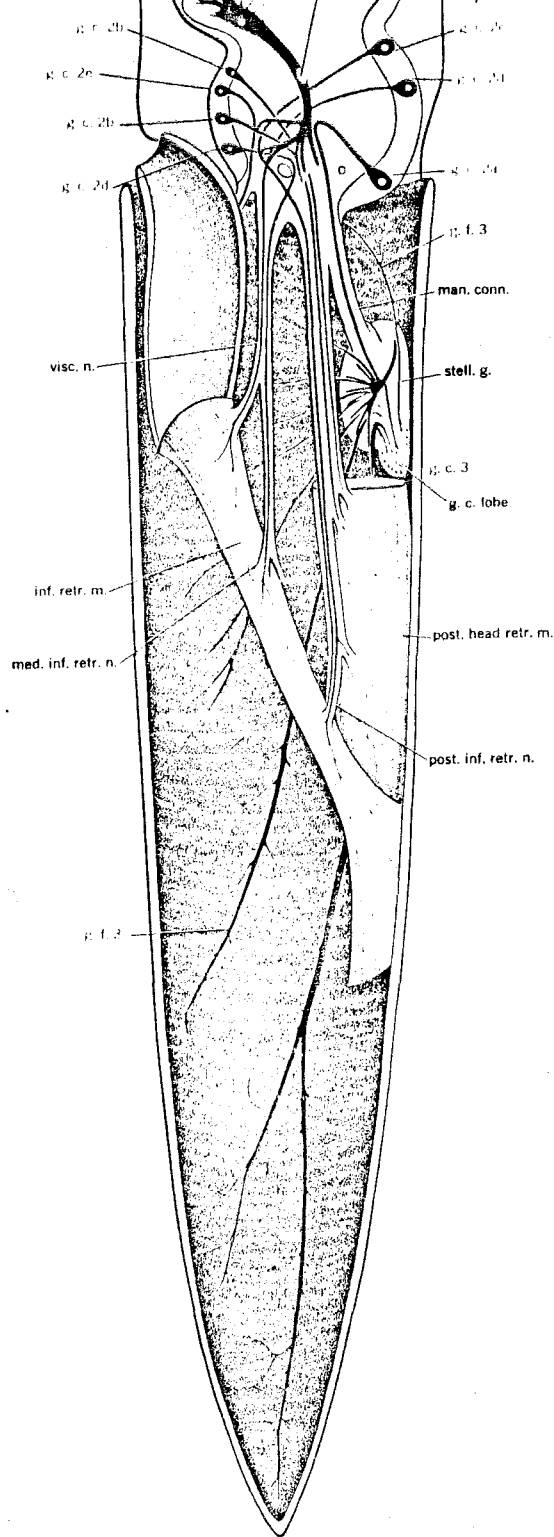


Fig.A.2. Diagram of the giant nerve fiber system of *Loligo Pealii*. br., interaxonic bridge; g.c.lobe, giant cell lobe; g.c.1, first-order giant cell; g.c.2a, second order giant cell whose axon runs to stellate ganglion and there makes the distal synapses; g.c.2b, second-order giant cell whose axon runs to the posterior head retractor muscle; g.c.2c, second-order giant cell whose axon runs to the same muscle and to the infundibulum retractor muscle; g.c.2d, second-order giant cell whose axon runs to the infundibulum retractor muscle; g.c.2e, second-order giant cell whose axon runs to the muscle; g.c.3, cells of origin of third-order giant fibers; g.f.3, third-order giant fiber, (from Bullock T.H. et al, 1965)

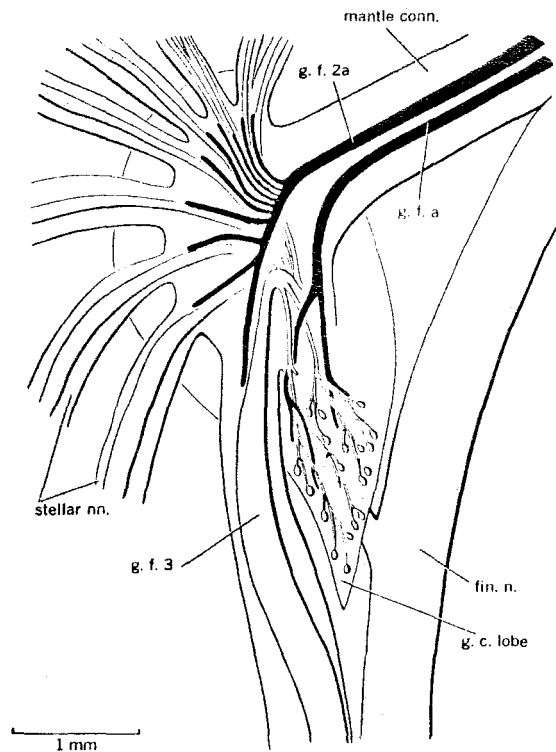


Fig.A.3. The giant fibers and their synapses and cell bodies in the stellate ganglion of *Loligo Pealii*; dimensions are to scale from a small specimen. fin.n., fin nerve—a division of pallial nerve of the brain; g.c.lobe, giant cell lobe; g.f.2a, second-order giant nerve fiber making the distal synapses on third-order giant fiber; g.f.a, giant fiber arising in the palliovisceral ganglion of the brain and making proximal synapses; g.f.3, third-order giant fiber; mantle conn., mantle connective—a division of the pallial nerve; stellar nn., stellar nerves, (from Bullock T.H. et al, 1965)

APPENDIX B

DIAGRAMS ILLUSTRATING FIXATION TABLE AND SPECIMEN HOLDER

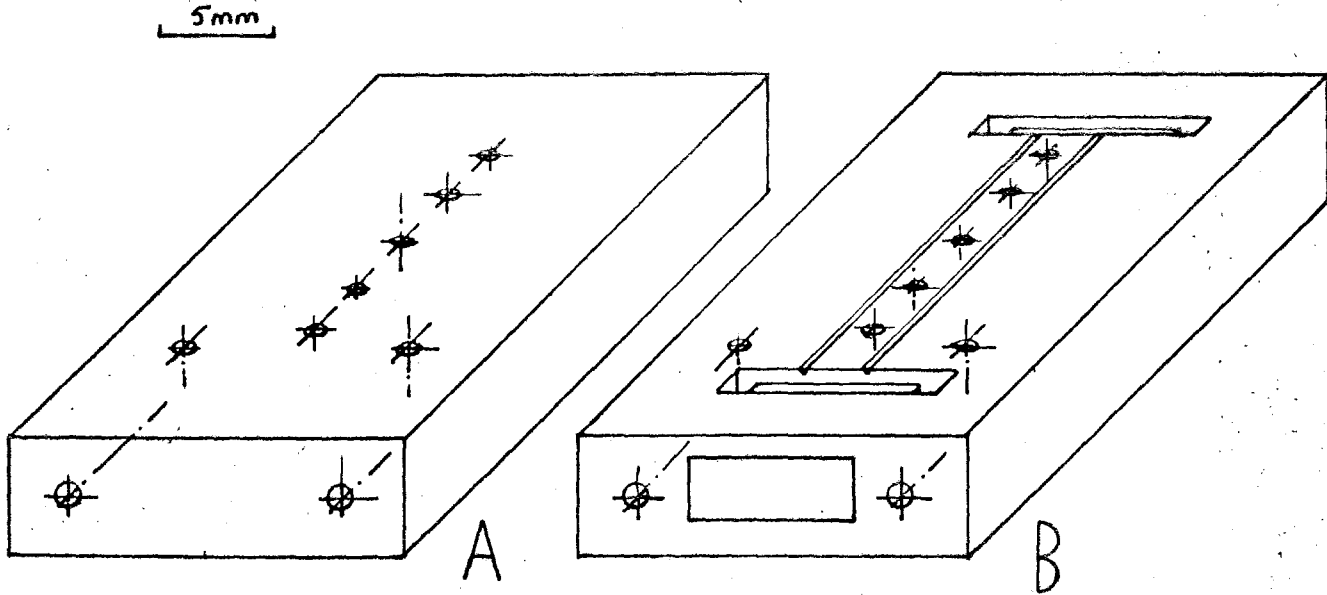


Fig.B.1. Diagram of fixation table made up of Plexiglass, drawn to scale. A: Intra-cellular portion, B: Extra-cellular portion.

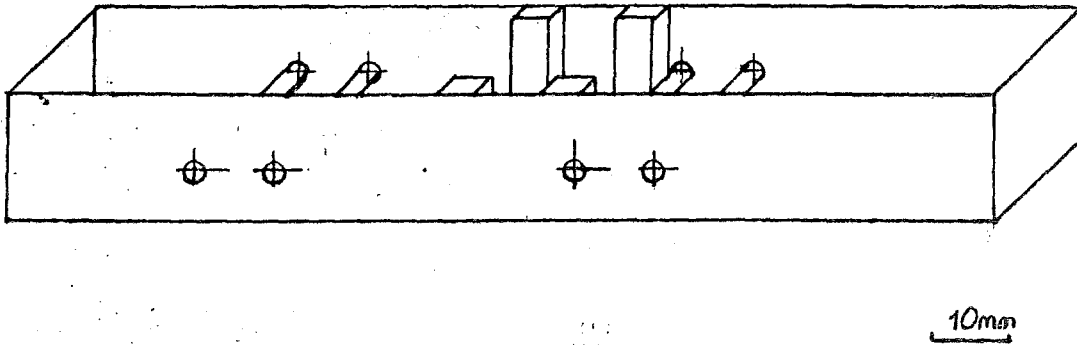


Fig.B.2. Diagram of specimen holder made up of Plexiglass, drawn to scale.

APPENDIX C

BLOCK AND PRINTED CIRCUIT DIAGRAMS OF DATA TRANSLATION BOARD

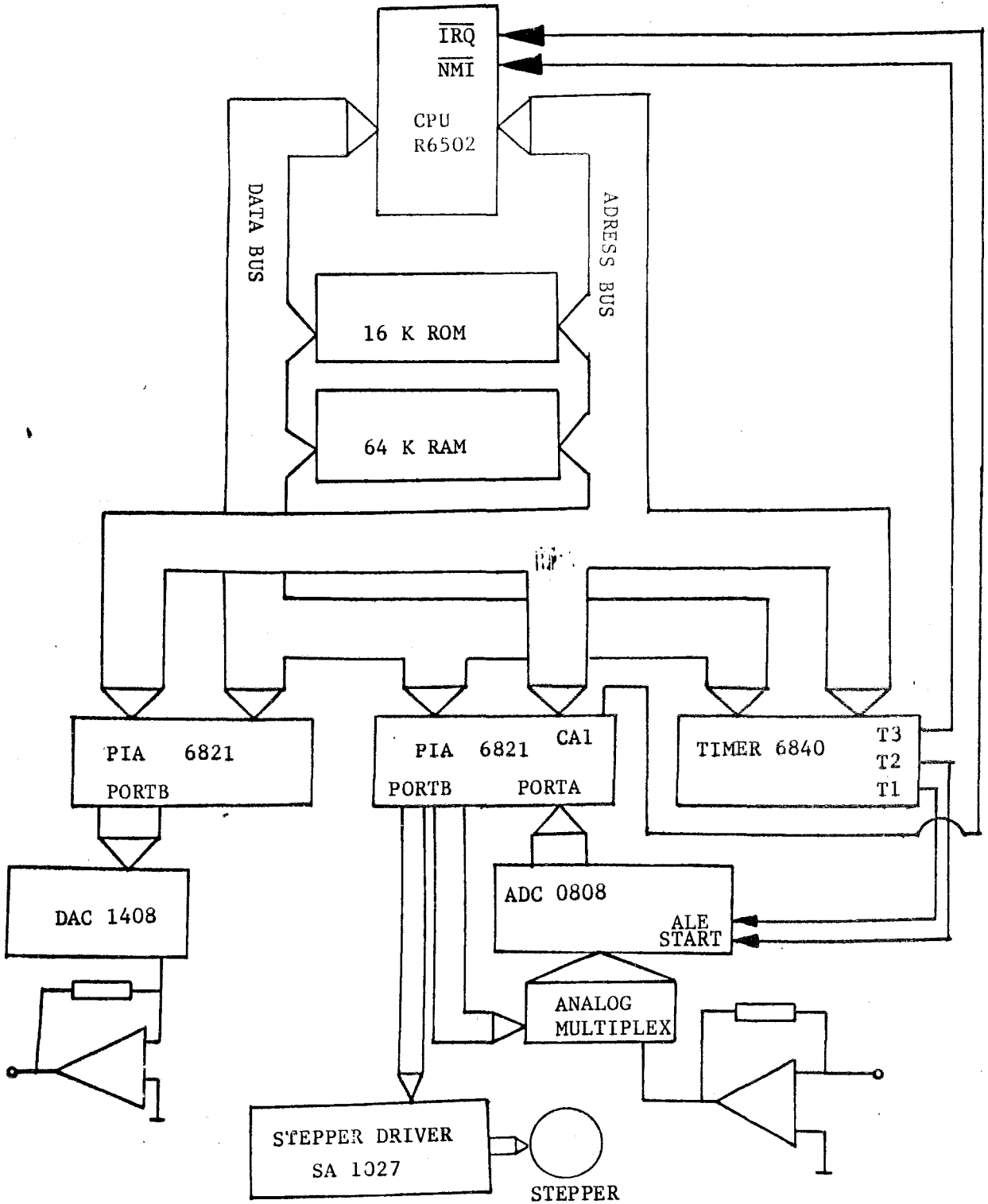


Fig.C.1. Block diagram of data translation.

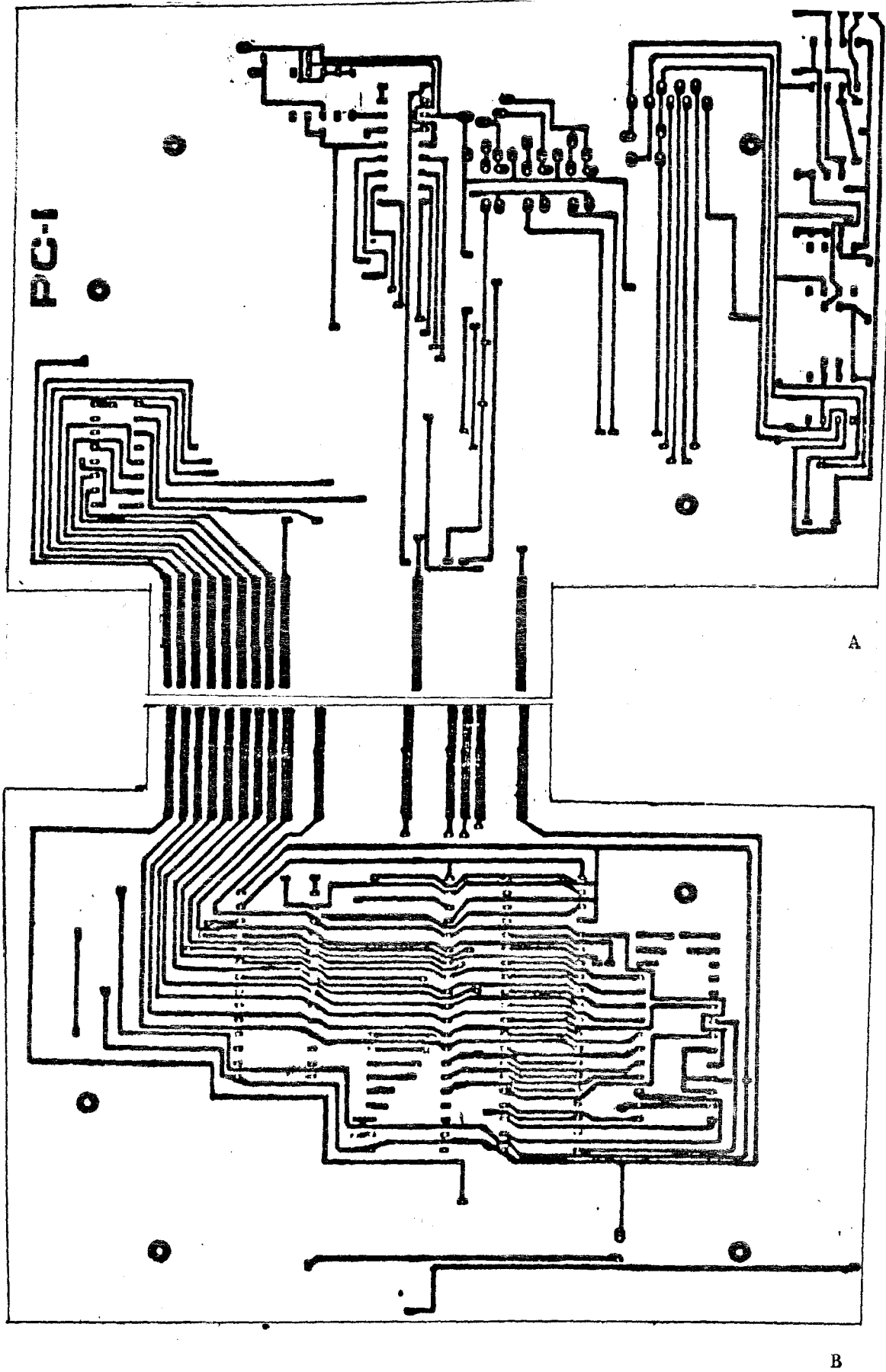


Fig.C.2. Printed circuit board diagram of data translation. A: Component side, B: PCB side.

APPENDIX D

MASTER PROGRAM LISTING

```
* The program is written in AppleSoft Basic language, therefore *
*
* for any modifications related to the program one must refer *
*
* to the AppleSoft Basic Reference Manual. *
```

```
10 HIMEM:8191
20 CLEAR:PRINT "FOR STYLUS ADJUSTMENT (PRESS <- FOR INWARD)":
   GOSUB 5000
30 PRINT "PRESS -> FOR OUTWARD, ENTER FOR O.K": CALL M2AIN
35 GET A#
40 IF ASC(A#)=8 THEN : POKE MOT,H1: POKE MOT,L1: POKE MOT,H1:
   GOTO 35
50 IF ASC(A#)=21 THEN: POKE MOT,H2: POKE MOT,L2: POKE MOT,H2:
   GOTO 35
60 IF ASC(A#) <> 13 GOTO 35
70 INPUT "GIVE TYPE OF EXCITATION (SIN,SQR,RAMP)": A#
80 IF A#="SIN" THEN GOSUB 1000: GOTO 110
90 IF A#="SQR" THEN GOSUB 2000: GOTO 110
100 IF A#="RAMP" THEN GOSUB 3000
110 INPUT "GIVE SAMPLING FREQUENCY (HZ)": FR: GOSUB 4000
120 PRINT "PRESS ANY KEY FOR BEGINNING"
130 GET A#
140 REM
150 REM
160 GOSUB 600: CALL M2AIN: CALL M10TR: CALL A4DC
```

```

170 PRINT "DO YOU WANT DATA TO BE SAVED(1), DISPLAYED ON CRT(2)":
PRINT "DISPLAYED ON SCOPE(3),PLOTTED BY A PLOTTER (4)":
PRINT "CONTINUE FOR ANOTHER CONVERSION WITH THE SAME
VARIABLES(5)":
PRINT "CONTINUE WITH DIFFERENT VARIABLES (6)": PRINT "END THE
PROGRAM(7)

180 INPUT "ENTER RELATED NUMBER "; A: ON A GOTO 200, 250, 350, 300,
400, 450, 500

190 GOTO 170

200 PRINT "WHEN READY FOR CASSETTE OUTPUT PRESS ANY KEY TO
CONTINUE": GET A#: POKE60,0: POKE 61,160: POKE 62,255:
POKE 63,191: CALL WRITE: GOTO 170

250 HOME: CALL CRT: GOTO 170

350 GOSUB 600: CALL M2AIN: POKE 17195,2: CALL D1AC: GOTO 170

400 GOTO 160

450 GOTO 20

500 END

600 POKE MOT+1,0: POKE DAC+1,0: POKE ADC+1,0: RETURN

* The subroutine calculating the Timer enable and Stepper motor *
* direction of rotation parameters and pokes them to the adress *
* 5000H consecutively by assuming the Sinus function composing *
* of discrete steps. *

1000 INPUT "GIVE FREQUENCY AND AMPLITUDE"; F, A
1010 INPUT "GIVE MINIMUM STEP SIZE"; A1
1020 X0= D2: T3= 0:D3= D2+8*A/A1: D4= D2+16*A/A1: X1= D4
1030 FOR I= 1 TO A/A1
1040 S= 1- I*I*A1*A1/(A*A): IF S=0 THEN: T= 0.25/F: GOTO 1060

```

```

1050 T= (ATN(I*A1/(A*SQR(S))))/(2*PI*F)
1060 T= T-T3: T3= T: GOSUB 4500
1070 POKE D2,H1: POKE D2+1,L1: POKE D2+2,T1: POKE D2+3,T2
1080 POKE D2+8*A/A1,H2: POKE D2+8*A/A1+1,L2: POKE D2+8*A/A1+2,T1:
      POKE D2+8*A/A1+3,T2
1090 POKE D3,T2: POKE D3-1,T1: POKE D3-2,L2: POKE D3-3,H2
1100 POKE D4,T2: POKE D4-1,T1: POKE D4-2,L1: POKE D4-3,H1
1110 D2= D2+4: D3= D3-4: D4= D4-4
1120 NEXT
1130 FOR I= X1+1 TO X0+256
1140 POKE I, PEEK (X0): X0= X0+1
1150 NEXT I
1160 RETURN

```

```

* The subroutine calculating the Timer enable and Stepper motor *
* direction of rotation parameters and pokes them to the adress *
* 5000H consecutively by assuming the Square function composing *
* of discrete steps. *

```

```

2000 INPUT "GIVE FREQ. AMPLITUDE & DC LEVEL"; F, A, DC
2010 INPUT " GIVE MIN. STEP SIZE & MAX. STEP RATE"; A1,SR
2020 T= 0.5/F: D3=D2+4*A/A1: D4=D2+8*A/A1+4: X0=D2: GOSUB 4500
2030 POKE D3,H1: POKE D3+1,L1: POKE D3+2,T1: POKE D3+3,T2
2050 T= 1/SR: D3=D3+4: GOSUB 4500
2060 FOR I=1 TO A/A1
2070 POKE D3,H1: POKE D3+1,L1: POKE D3+2,T1: POKE D3+3,T2
2080 POKE D3,H2: POKE D3+1,L1: POKE D3+2,T1: POKE D3+3,T2

```

```

2090 D2=D2+4: D3=D3+4: NEXT I
2100 FOR I= D4+4 TO X0+256
2110 POKE I, PEEK (X0): X0= X0+1
2120 NEXT I
2130 IF DC < 0 THEN: FOR I=1 TO ABS(DC)/A1: POKE MOT,H2: POKE
      MOT,L2: NEXT: RETURN
2140 IF DC > 0 THEN: FOR I=1 TO DC /A1: POKE MOT,H1: POKE
      MOT,L1: NEXT: RETURN
2150 RETURN

```

```

* The subroutine calculating the Timer enable and Stepper motor *
* direction of rotation parameters and pokes them to the address *
* 5000H consecutively by assuming the Ramp function composing of *
* discrete steps. *

```

```

3000 INPUT "GIVE RAMP TYPE (1) FOR IN, (2) FOR OUT"; TY
3100 INPUT "GIVE MIN. STEP SIZE, AMPLITUDE, RISE TIME"; A1, A, F
3020 T= F*A1/A: GOSUB 4500: X0=D2
3030 ON TY GOTO 3040, 3080
3040 FOR I= 1 TO A/A1
3050 POKE D2,H2: POKE D2+1,L2: POKE D2+2,T1: POKE D2+3,T2
3060 D2= D2+4: NEXT I: X1= D2
3070 POKE D2,L2: POKE D2+1,L2: POKE D2+2,255: POKE D2+3,255:
      GOTO 3120
3080 FOR I= 1 TO A/A1
3090 POKE D2,H1: POKE D2+1,L1: POKE D2+2,T1: POKE D2+3,T2
3100 D2= D2+4: NEXT I: X1= D2
3110 POKE D2,L1: POKE D2+1,L1: POKE D2+2,255: POKE D2+3,255:
3120 FOR I= X1+4 TO X0+256

```

3130 POKE I, PEEK (X1): X1= X1+1

3140 NEXT I:RETURN

* The subroutine calculating the NMI periods to drive the Step- *
* per. The NMI period is determined by the value written on the *
* Timer latches. *

4000 T= 1E6/FR: T2=255

4010 T1= T/T2-1: IF ABS ((INT(T1)+1)*(T2+1)-T) >1 THEN: T2=T2-1:
GOTO 4010

4020 IF T1>T2 THEN 4040

4030 POKE M2+1,T1: POKE M2+9,T2-1: RETURN

4040 PRINT " NOT FOUND ": STOP: RETURN

* The subroutine calculating the Timer output periods that drive*
* the ADC. The IRQ period generated by ADC is determined by the *
* values written on Timer latches. *

4500 T1= INT(T*1E6/256): IF T1>255 GOTO 4530

4510 T2= INT((T*1E6/256-T1)*255

4515 IF T<0.008 GOTO 4530

4520 RETURN

4530 PRINT " NOT FOUND ": STOP: RETURN

* The responsible addresses given in decimal for relevant *
* locations and machine language subroutines. *

5000 M2AIN= 16384: MDT= 49370: DAC= 49352

5010 M1OTR= 16896: A4DC= 16640: ADC= 49366

5020 WRITE= 60570: D1AC= 17152: D2= 20480

5030 CRT= 17408: PI= 3.1416: H1= 32: H2= 96: L1= 0: L2= 64

5040 RETURN

APPENDIX E
 CD-PROGRAM LISTINGS

```
* The decoded beginning addresses for two PIAs (M6821) and for
*
* TIMER (M6840) are COCBH, CODBH and COD0H respectively. The ADC
*
* lies in the address of CODBH (PIA1DRA) while CODAH is the
*
* address of STEPPER's direction and rotation , and ADC's
*
* channel multiplexing pins beginning respectively from LSB.
*
* The address COCBH holds the PIA2DRA which drives DAC. All the
*
* intermediate addresses for PIA's and for TIMERS are chip
*
* dependent and are available in Microprocessors Data Manual,
*
* MOTOROLA, Inc. The specifications for DAC1408 and ADC0808 are
*
* available in Linear Data Book, NATIONAL SEMICONDUCTORS, Inc.
```

```
M2AIN          LDA #03          ;The routine to initialize ports
                STA COD2
                STA COD4
                LDA #F8
                STA COD3
                STA COD5
                LDA #FF
                STA COD6
                LDA #FF
                STA COD7
                LDA #00
                STA COD8
                LDA #07
                STA COD9
                LDA #FF
                STA CODA
                STA COC9
                LDA #43
                STA COD0
                LDA #87
                STA COD1
                STA COD0
                RTS
```

```
A4DC          JSR 4160
                LDA C05B          ;RAM bank switch on
                LDY #FF
                LDA 0000,Y        ;save zero page
```



```

        STA C100,Y
        LDA 0100,Y      ;save stack
        STA C200,Y
        DEY
        BNE 410B
        LDA C05A      ;RAM bank switch off
        LDX #FF
        TSX
        LDA #80       ; IRQ/256
        STA 03FE      ; IRQ vector LSByte
        LDA #41       ; IRQ
        STA 03FF      ; IRQ vector MSByte
        LDA #00
        STA 3C
        LDA #A0
        STA 3D
        LDA #C0
        STA 3E
        CLI
        LDA #86
        STA C0D0      ; Enable TIMERS
        LDA 3D
        CMP 3E
        BNE 4139      ; Loop until data input buffer full
        LDA #87
        STA C0D0      ; Stop TIMERS
4144:   LDA C05B      ; Routine for turning back to
        LDY #FF      ; Master Program
        LDA C100,Y
        STA 0000,Y
        LDA C200,Y
        STA 0100,Y
        DEY
        BNE 4149
        LDA C05A
        JSR 4170
        RTS

4160:   STA E5       ; Register saving routine
        STX E6
        STY E7
        PHP
        PLA
        STA E8
        TSX
        STX E9
        RTS

4170:   LDX E9       ; Register retrieving routine
        INX
        INX
        TXS
        LDA E8
        PHA
        PLS

```

```

LDY E7
LDX E6
LDA E5
RTS

```

```

4180: ADCIRQ      SEI                ; The IRQ servicing routine which
                  PHA                ; reads data from ADC via PIA and
                  LDY #00            ; saves it to the data buffer
                  LDA COD8          ; A000H - BFFFH
                  STA (3C)Y
                  LDA 3C
                  CLC
                  ADC #01
                  STA 3C
                  LDA 3D
                  ADC #00
                  STA 3D
                  PLA
                  RTI

```

```

M10TR (4200H):  LDA #4C                ; JMP opcode
                  STA 03FB
                  LDA #80
                  STA 03FC          ; NMI vector LSByte
                  LDA #42
                  STA 03FD          ; NMI vector MSByte
                  LDY #00
                  STY 47
                  RTS

```

```

MOTNMI:        SEI                ; The NMI servicing routine to drive
                  PHA                ; the STEPPER by its direction and
                  PHP                ; step codes and also generating the
                  TYA                ; next NMI period by writing to the
                  PHA                ; TIMER latches
                  LDY 47
                  LDA 5000,Y
                  STA CODA
                  INY
                  LDA 5000,Y
                  STA CODA
                  INY
                  LDA 5000,Y
                  STA COD6
                  INY
                  LDA 5000,Y
                  STA COD7
                  INY
                  STY 47
                  PLA
                  TAY
                  PLP
                  PLA

```

RTI

```
D1ADC (4300H): LDA #4C      ; The routine to enable Timers to
                STA 03FB    ; generate NMI periods for data
                LDA #80    ; output from data buffer A000H -
                STA 03FC    ; BFFFH via DAC
                LDA #43
                STA 03FD
                LDA #00
                STA 3C
                LDA #A0
                STA 3D
                LDA #C0
                STA 3E
                LDA #00
                STA COD1
                LDA #42
                STA COD0
                LDA #01
                STA COD1
                LDA #05
                STA COD6
                LDA #FF
                STA COD7
                LDY #00
                SEI
                LDA #00
                STA COD0
                LDA 3D
                CMP 3E
                BNE 433C
                JSR 4144
```

```
DACNMI:        PHA          ; NMI servicing routine for
                LDA (3C)Y    ; data output
                STA COCB
                LDA 3C
                CLC
                ADC #01
                STA 3C
                LDA 3D
                ADC #00
                STA 3D
                CMP 3E
                BNE 439E
                LDA #01
                STA COD1
                PLA
                RTI
                LDA 432B
                STA COD6
                LDA #FF
                STA COD7
```

PLA
RTI

*
* This subprogram uses built in screen RAM area which is bit- *
* mapped. This area's beginning adress is 2000H and the problem *
* associated with the mapping causes to manipulate some arith- *
* metic operations. For a descriptioal mapping see fig.E.1. *
* This routine retrieves data from A000H-BFFFH and displays it. *
*
*

LDA #00	LSR
STA 3C	LSR
STA 3E	PHA
STA 40	BCC 4450
STA 22	LDA #80
LDA #20	CLC
STA 30	ADC 3C
STA 3F	STA 3C
LDA #A0	PLA
STA 41	ADC 3D
LDA #C0	STA 3D
STA 42	TYA
LDA #08	AND #07
STA 23	ASL
LDA 3E	ASL
STA 20	ADC 3D
CLC	STA 3D
ADC #01	LDA 43
STA 21	LDY #00
JSR FC58	ADC (3C)Y
LDA #01	STA (3C)Y
STA 43	INC 40
LDY #00	BNE 4472
LDA (40)Y	INC 41
EOR #FF	LDA 42
LSR	CMF 41
LSR	BEQ 4484
TAY	ASL 43
LDA 3E	BCC 442C
STA 3C	INC 3E
LDA 3F	LDA #28
STA 3D	CMF 3E
TYA	BNE 441C
AND #38	LDA #00
BEQ 4455	STA 3E
LSR	BEQ 441C
LSR	LDA #00

```

STA 20
LDA #28
STA 21
LDA #18
STA 23
RTS

```

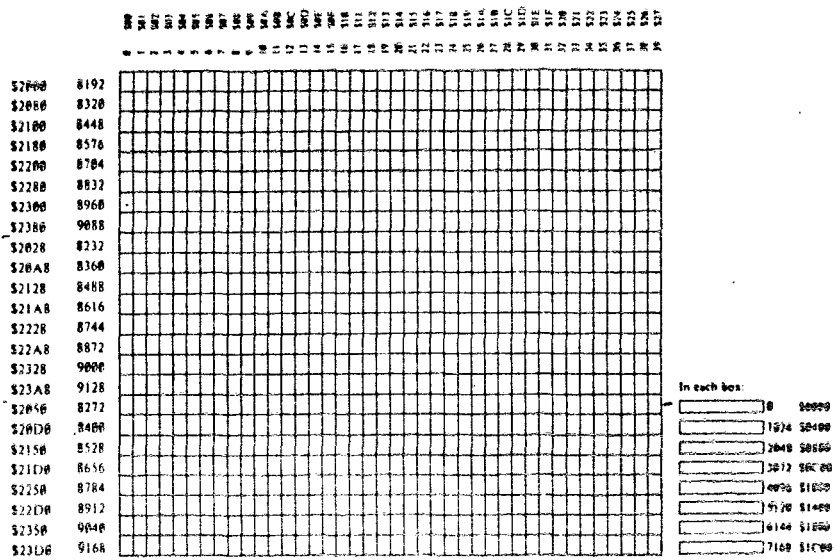


Fig.E.1 Map of high resolution graphics mode

APPENDIX F

OUTLINES OF CALCULATION OF DEFORMATION DISTRIBUTION
 IN A CIRCULAR MEMBRANE
 DEFORMED BY A STYLUS

Assuming the membrane has to overcome the intrinsic forces given in fig.E.1, the general elastic curve equation can be applied to this membrane which is

$$\frac{d^2 z}{dx^2} = \frac{- M_e}{E I} \quad (E.1)$$

where E is the elasticity constant, I is the moment of inertia. The bending moment Me, can be expressed as;

$$M_e = \frac{F d\phi}{2\pi} x \quad (E.2)$$

and the moment of inertia

$$I = \frac{(R-x) \delta^3 d\phi}{12} \quad (E.3)$$

where δ is the thickness of the membrane, F is the applied force, R is the diameter of the circular membrane, r is the diameter of the stylus. The boundary conditions for the eq. E.1 is :

$$x = R-r \quad \frac{dz}{dx} = 0 \quad (E.3a)$$

$$x = 0 \quad z = 0 \quad (E.3b)$$

By substituting Eq. E.2. and Eq. E.3 to Eq. E.1

$$\frac{d^2 z}{dx^2} = \frac{- \delta F}{E \pi \delta^3} \left(\frac{x}{R-x} \right) \quad (E.4)$$

where it is evident that the elastic curve is independent of angle. By integrating this equation twice and by taking into consideration the boundary conditions E.3a and E.3b and by arranging elastic curve equation can be found as;

$$z = \frac{\Delta F}{E\pi\delta^3} \left[\frac{x^2}{2} - (2R-r)x - Rx \ln \left| \frac{r}{R-x} \right| - R^2 \ln \left| \frac{R}{R-x} \right| \right] \quad (E.5)$$

This equation is invalid when $x > R-r$ since the membrane under the stylus mustnot be deformed because of the stiffness of the stylus. Therefore the region between $R-r < x < R$ is to be considered as a solid line parallel to x axis. The z coordinate of the function of elastic curve can be calculated by substituting $R-r$ to the expression E.5 instead of x . The deformation distribution of the membrane can be expressed as:

$$f(x) = \frac{S(x)}{x} \quad (E.6)$$

where $S(x)$ is the line integral of elastic curve and can be given as

$$S(x) = \int \sqrt{1 + z'^2} \, dx \quad (E.7)$$

Where

$$z' = \frac{-\Delta F}{E\pi\delta^3} [R-x - R \ln |R-x| + R \ln |r| - r] \quad (E.8)$$

The solution of this integral can be done by numerical methods. Thus spatial deformation distribution of the membrane resulting from the peak change can be evaluated.

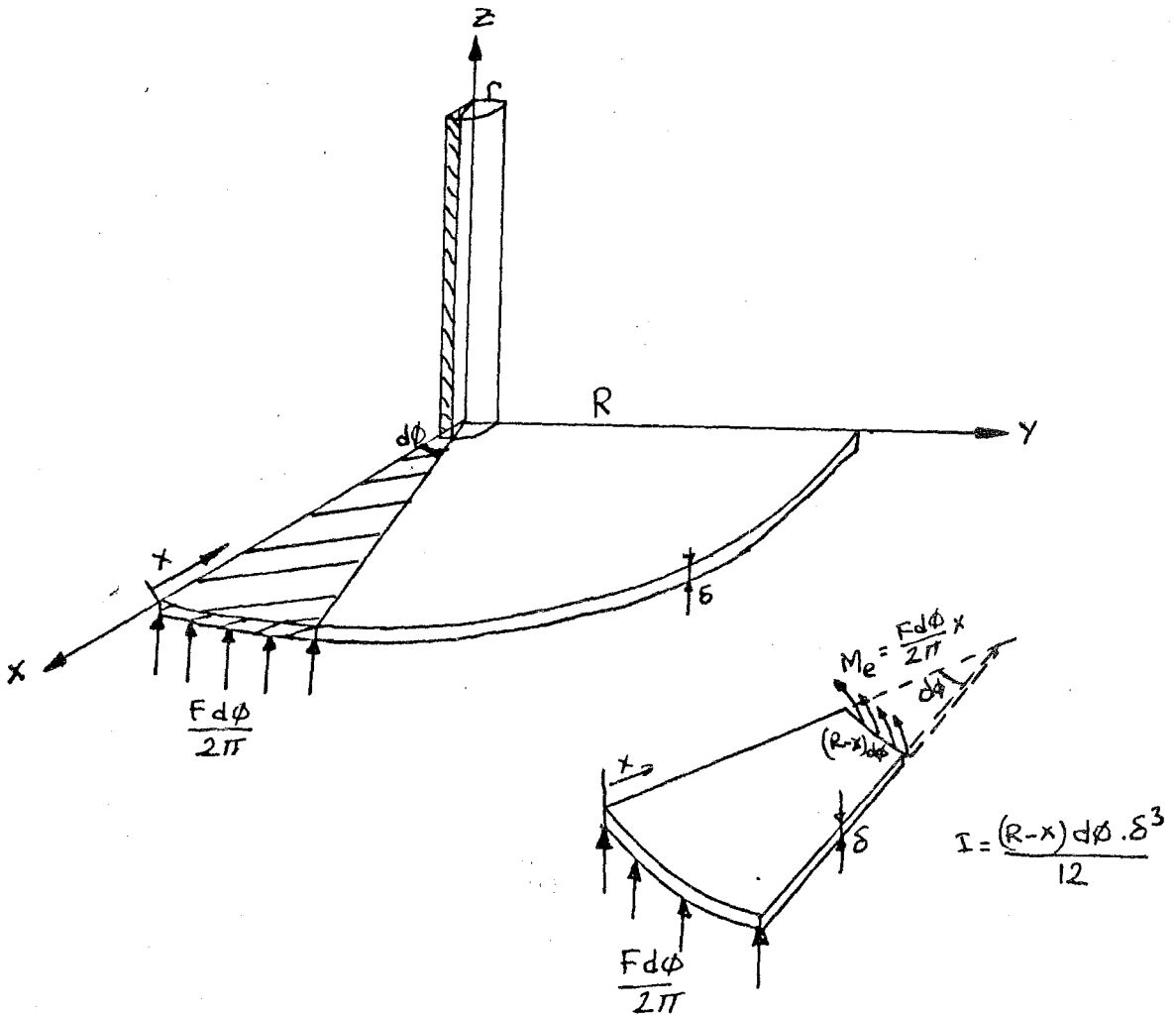
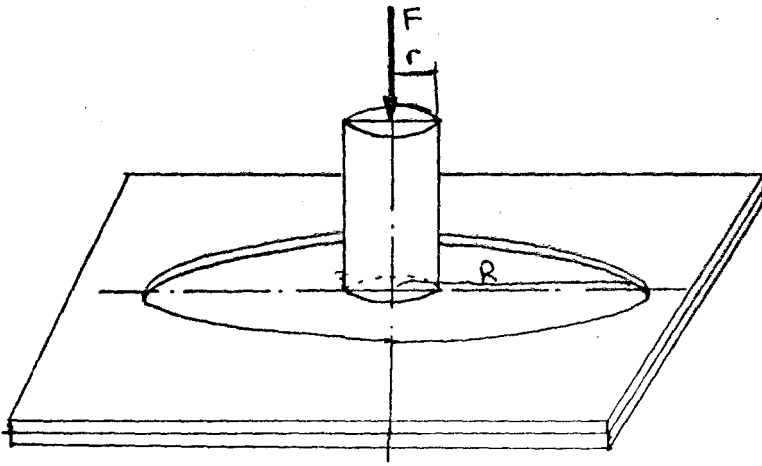


Fig.E.1. A schematic of the circular membrane showing intrinsic forces and moments.

BIBLIOGRAPHY

1. ARNDT J.O., DORRENHAUS A., WIECKEN H. (1975) The aortic arch baroreceptor response to static and dynamic stretches in an isolated aorta-depressor nerve preparation of cats In Vitro. J.Physiol., 252:59-78
2. BAKER P.F., HODGKIN A.L., SHAW T.I. (1962a) The effects of changes in internal ionic concentrations on the electrical properties of perfused giant axons. J.Physiol., 164:355-374
3. BAKER P.F., HODGKIN A.L., SHAW T.I. (1962b) Replacement of axoplasm of giant nerve fibres with artificial solutions. J.Physiol., 164:330-337
4. BERGEL D.H., BERTHAM C.D., BROOKS D.E., MACDERMOTT A.J., ROBINSON J.L., SLEIGHT P. (1975) Simultaneous recording of the carotid sinus dimensions and the baroreceptor nerve in the anaesthetized dog. Proc. Physiol.Soc., 252:15-16p
5. BINSTOCK L., GOLDMAN L., (1967) Giant axon of *Myxicola*: some membrane properties as observed under voltage-clamp. Science, 158:1467-1469
6. BINSTOCK L., GOLDMAN L., (1969) Current- and voltage-clamped studies on *Myxicola* Giant axons. J.Gen.Physiol.(London), 54:730-742
7. BREHM P., KULLBERG R., MOODY-CORBETT F. (1984) Properties of non-junctional acetylcholine receptor channels on innervated muscle of *Xenopus laevis*. J. Physiol., 350:631-648
8. BULLOCK T.H. (1965) Structure and function in the nervous systems of invertebrates Vol:2. Ed. by Bullock T.H. & Horridge G.A., Freeman Book Co., San Francisco
9. COREY D.P., HUDSPETH A.J (1979) Ionic basis of the receptor potential in a vertebrate hair cell. Nature, 281:675-677
10. EVANS E.A., SKALAK R. (1980) Mechanics and thermodynamics of biomembranes. CRC Press, Florida
11. FLOCK A. (1965) Transducing mechanisms in lateral line canal organ receptors. Cold Spring Harbor Symp. Quant. Biol., 30:133-146
12. GANOT G., WONG B., BINSTOCK L., EHRENSTEIN G. (1981) Reversal potentials corresponding to mechanical stimulation and leakage currents in *Myxicola* giant axon. Biochim.Biophys.Acta, 649:487-491
13. GUZELSU N. (1985) Electromechanical properties and

electromagnetic stimulation of bones. Biomedical Engineering Institute Publications, Istanbul.

14. GOTO K. (1983) Transmembrane macromolecule rotation model. Tohoku J. exp. Med., 139:159-164

15. GROSS D., WILLIAMS W.S., CONNOR J.A. (1983) Theory of electro-mechanical effects in nerve. Cellular and Molecular Neurobiology, 3:89-111

16. GUHARAY F., SACHS F. (1984) Stretch-activated single ion channel currents in tissue cultured embryonic chick skeletal muscle. J. Physiol., 352:685-701

17. GUHARAY F., SACHS F. (1985) Mechanotransducer ion channels in chick skeletal muscle: The effects of extracellular pH. J. Physiol., 363:119-134

18. GURKAN S.I., SANDALLI P., BAYIRLI G. (1972) Dis hastalıkları ve konservatif tedavisi. Bozak Yayınevi, Istanbul

19. HAMILL O.P., NEHER E., SAKMANN B., SIGWORTH F.J. (1983) Reprints from single channel recordings. Plenum Press., N.Y.

20. HAMILL O.P. (1983) Potassium and chloride channels in red blood cells. Reprints from single channel recording. Plenum Press., N.Y.

21. HARRISON R., LUNT G.G. (1980) Biological membranes, Blackie & Son press, 2nd edition, Glasgow, London.

22. HILLMAN D.E. (1971) Morphological basis for a mechanical linkage in otolithic receptor transduction in the frog. Science, 174: 416-419

23. HOFFMAN J.F. (1975) Ionic transport across the plasma membrane. Cell Membranes, biochemistry, cell biology & pathology., Edit. by Weismann G. & Claiborne R., HP Publishing Co., NY.

24. HODGKIN A.L., HUXLEY A.F. (1952) A quantitative description of membrane current and its application to conduction and excitation in nerve. J. Physiol., 117:500-544

25. HUNT C.C., WILKINSON R.S. (1980) An analysis of receptor potential and tension of isolated cat muscle spindles in response to sinusoidal stretch. J. Physiol., 302:241-262

26. ILYINSKY O.B. (1965) Process of excitation and inhibition in single mechanoreceptors (Pacinian Corpuscle). Nature, 208:351-353

27. JULIAN F.J., GOLDMAN D.E. (1962) The effects of mechanical

- stimulation on some electrical properties of axons. J.Gen.Physiol. (London), 46:297-313
28. KUKITA F., YAMAGISHI S. (1983) Effects of outward water flow on potassium currents in a squid giant axon. J. Membrane Biol., 75 :33-44
29. LENZ J.E., KELLY E.F. (1980) A potential difficulty in A/D conversion using microcomputer system. IEEE Trans. Biomed. Eng., 27:668-669
30. LLANO I., BEZANILLA F. (1984) Analysis of sodium current fluctuations in the cut-open squid giant axon. J.Gen.Physiol. (London), 83:133-142
31. LOEWENSTEIN W.R., TERZUOLO C.A., WASHIZU Y. (1963) Separation of transducer and impulse-generating processes in sensory receptors. Science, 142:1180-1181
32. LOWENSTEIN O., WERSALL J. (1959) A functional interpretation of the electron-microscopic structure of the sensory hairs in the cristae of the elasmobranch Raja Clavata in terms of directional sensitivity. Nature, 184:1807-1808
33. MATSUMOTO G. (1984a) A proposed membrane model for the generation of sodium currents in squid giant axons. J.Theor. Biol., 107:649-666
34. MATSUMOTO G., ICHIKAWA M., TASAKI A. (1984b). J.Membrane Biology, 77:93
36. MULROY M.J., WHALEY E.A. (1984) Structural changes in auditory hairs during temporary deafness. Scanning Electron Microscopy, 2:831-840
37. NAITOH Y., ECKERT R. (1973) Sensory mechanisms in Paramecium. J. Exp.Biol., 59:53-65
38. NISHI K., SATO M. (1968) Depolarizing and hyperpolarizing receptor potentials in the non-myelinated nerve terminal in Pacinian corpuscles. J.Physiol., 199:383-396
39. OHMORI H. (1985) Mechano-electrical transduction currents in isolated vestibular hair cells of the chick. J.Physiol., 359:189-217
40. POPPELE R.E., KENNEDY W.R., QUICK D.C. (1978) A determination of static mechanical properties of intrfusar muscle in isolated cat muscle spindles. Neuroscience, 4:401-411

41. SINGER S.J. (1975) Architecture and topography of cell membranes. Cell Membranes, biochemistry, cell biology & pathology., Edit. by Weismann G. & Claiborne R., HP Publishing Co., NY.
42. SNIK A.F.M., BEUMER T.A.M., POULIS J.A. (1982) Measurements of the elasticity of monolayers consisting of lipids from nerve membranes. Biochim. Biophys. Acta., 689:346-350
43. TASAKI I., IWASA K., GIBBONS R.C. (1980a) Mechanical changes in crab nerve fibres during action potentials. Jpn.J.Physiol., 30 :987-905
44. TASAKI I., IWASA K., GIBBONS R.C. (1980b) Swelling of nerve fibres associated with action potentials. Science, 210 :338-339
45. TASAKI I., IWASA K. (1982) Further studies of rapid mechanical changes in squid giant axon associated with action potential production. Jpn.J.Physiol., 32:505-518
46. TERAKAWA S., WATANABE A. (1982) Electrical responses to mechanical stimulation of the membrane of squid giant axons. Pflugers Arch., 395:59-64
47. TIGERSTEDT R. (1880) Studien uber die mechanischen Nervenreizung ,Helsingfors, Druckerei der Finnischen Literatur Gesellschaft